SLAC – PUB – 3928
April 1986
(T/E)

FUTURE FRONTIERS FOR e^+e^- COLLISIONS: PHYSICS OF SLC AND LEP*

JONATHAN M. DORFAN

Stanford Linear Accelerator Center
Stanford University, Stanford, California 94305

TABLE OF CONTENTS

*Work supported by the Department of Energy, contract DE–AC03–76SF00515.

Lectures given at the Lake Louise Winter Institute on New Frontier in Particle Physics, Lake Louise, Canada, February 16-22, 1986

1. INTRODUCTION

This report summarizes three lectures given at the Lake Louise Winter Institute on New Frontiers in Particle Physics. The audience comprised about 25% graduate students in high energy particle physics, 20% low and medium energy physicists and the remainder Ph.D's involved in high energy particle physics. I was asked to set the level of the lectures such that it would be of benefit to the two former groups. This report reflects strongly the level at which I lectured and I have made no attempt to broaden the scope for this writeup. The lectures are based on two previous lecture series which I gave[1] and I have borrowed liberally and directly from these reports.

The theme of the Winter School at Lake Louise was the future frontiers in particle physics. My job was to present the e^+e^- frontier, which I chose to define as the physics which will be done at the SLC and LEP. I placed considerably more emphasis on the Z^0 physics than the higher energy running – although the important high energy tests are covered. For a more complete discussion of the high energy LEP physics program the reader is referred to reference 2. John Ellis's lectures at this school cover the search for Higgs and SUSY particles in great detail. They should be considered as supplementary to what is discussed here – in particular his discussion of SUSY searches is much more thorough.

The outline of these lectures is as follows. We begin with a brief historical review of the contribution to particle physics of e^+e^- interactions and the advantages of this laboratory. This is followed by a discussion of the LEP and SLC machines and the reasons for developing linear colliders. A brief overview of the Standard Model and some essential formalism for the process $e^+e^- \to f\bar{f}$ are presented, followed by a discussion of detectors. Next we look at how tests of the Standard Model and physics beyond the Standard Model can be made running at the Z^0. Finally, LEP physics at energies above the Z^0 is discussed.

2. HISTORICAL PERSPECTIVE

The next frontier in e^+e^- interactions is "just around the corner" with the impending commissioning of the Z^0 "factories" SLC at SLAC (fall 1986) and LEP at CERN (fall 1988). These machines will provide copious ($\sim 10^6$ per year) production of Z^0's and we will explore here why this frontier promises to be so exciting. Following the physics of the Z^0, the next planned e^+e^- frontier will be provided by upgrading the energy of the LEP machine. By adding conventional RF, LEP can be pushed to a center-of-mass energy ($E_{c.m.}$) of $\lesssim 170$ GeV and by adding superconducting RF, upwards of 200 GeV is possible. To go substantially beyond $E_{c.m.} = 200$ GeV with e^+e^- interactions will require building a large-scale linear collider. It is too early to propose such a machine. We need to see how well the prototype for this machine (the SLC) works and what we learn in the next few years about where the next interesting frontier lies. There are many technical problems with building high luminosity, high energy linear colliders. These technical problems require many years of study before a sensible design will emerge.

During the past 15 years, e^+e^- colliding beam facilities have served as important frontiers in our quest for a better understanding of the forces of nature. Many discoveries and considerable elucidation have come from the e^+e^- colliding beam machines. A short, and by no means complete, history is illustrative. During the early to mid 1970's the e^+e^- colliding beam machines CEA, FRASCATI, SPEAR and DORIS provided a dazzling array of discoveries and an impressive list of measurements. These include: 1) the measurement of $R = \sigma_{\text{hadrons}}/\sigma_{\mu^+\mu^-}$ which provided verification that quarks come in three colors, 2) the discovery of the charm quark which verified the GIM mechanism and provided a (shortlived) equality between the number of quarks and leptons, 3) the discovery of the τ lepton which indicated the presence of a 3rd generation, 4) the discovery of jets which added more credence to the notion of spin 1/2 quarks, 5) the discovery of open charm, both charmed mesons and baryons, and 6) the study of $c\bar{c}$ spectroscopy and the discovery of the χ_c states, which provided important tests of potential models. Following the discovery of the b quark in fixed target experiments, the CESR and DORIS II machines were able to contribute: 1) careful studies of the $b\bar{b}$ spectroscopy including the discovery of the higher Υ resonances and the χ_b states, 2) the discovery of bottom mesons, 3) an impressive set of measurements on weak decays which provide valuable input for the structure of the weak mixing matrix, 4) the absence of flavor changing neutral currents which imply that the t quark must exist as a partner for the b quark (the B_L quark cannot exist as a singlet), and 5) a precision measurement of $\Lambda_{\overline{MS}}$ which is an important test of QCD. Studies during the 1980's at PETRA, DORIS II, CESR, PEP and SPEAR have provided 1) clear evidence of 3 jet events which provides

strong evidence of the validity of QCD and is often quoted as the "discovery of the gluon", 2) verification of the Electro-Weak Theory from measurements of $\mu^+\mu^-$ and $\tau^+\tau^-$ charge asymmetries, 3) vast body of tests of QCD including clear evidence for scaling violations in particle momentum distributions, measurements of $\alpha_s(\Lambda_{\overline{MS}})$ and first indications that, as predicted by QCD, quarks and gluons fragment differently, 4) first measurements of the τ (known now to 10%) lifetime which provides an important test of τ/μ universality, 5) first measurement of the (surprisingly long, $\sim$ 1 picosecond) b quark lifetime which provides important constraints for the weak mixing matrix, 6) measurements of the D^o, D^+ and F lifetimes, 7) most comprehensive study of quark fragmentation which provides considerable input for model building and non-perturbative QCD, 8) vast number of (negative) searches for light techni-pions, charged Higgs, SUSY "anythings", top quark, monojets, 4th generation quarks and leptons..., and 9) discovery of unexpected states $\theta(1420)$, $\iota(1640)$ and $\xi(2200)$ with implications that some of these could be "glueballs" (particles made up of two gluons in a color singlet).

This catalog is impressive and is testament to the fact that e^+e^- colliders provide an ideal frontier environment. This is mainly because they offer:

1. Clean production of natures' fundamental building blocks – the quarks and leptons. This is typically in the form of pair production of the fermion and anti-fermion.
2. All the center-of-mass energy is available for the production of these fundamental building blocks. This can be contrasted with pp (or $\bar{p}p$) collisions where hard collisions between two constituents happen at an (unknown) energy typically $\lesssim 1/6$ of the available energy. The 4 quarks not involved in the collision provide debris which render study of the hard constituent collision very difficult – the pp environment is not "clean".
3. Because the e^+e^- environment is so clean, there is an enormous potential for discoveries and in-depth study of phenomena as was justified in the previous paragraph.

At the same time it should be acknowledged that, to move beyond the planned frontiers at SLC and LEP, one encounters major technical problems with the e^+e^- colliders. Firstly, as $E_{c.m.}$ is raised, the cross section is dropping (like $E_{c.m.}^{-2}$) and correspondingly higher luminosities are required. Whereas the pp technology can be scaled up to $\gtrsim 1$ TeV effective collision energy, the scaling laws for the e^+e^- colliders for that energy range are extremely demanding and enumerable technical problems are still to be solved. The present technology cannot be scaled up – new accelerator technologies are needed.

If we consider our present theoretical understanding of nature, where does it indicate that we should be planning our next frontier? Our present understanding of the three basic particle interactions – strong, weak and electromagnetic – is

in terms of the so-called Standard Model of $SU(2) \wedge U(1) \wedge SU(3)_{\text{color}}$. This model has been enormously successful at explaining all data at presently available energies. The absence of significant conflicts between the Standard Model and experiment is most impressive. To be sure, there are some essential ingredients of the Standard Model as yet unobserved – the top quark and the neutral Higgs. But their experimental absence in no way threatens the model. With this "happy" situation, why do we need a new frontier? Perhaps a sharper way to state this would be to ask "what do we expect to learn from experiments at a higher energy frontier?"

There are many reasons to push to higher energies, three of which are:

1. Most theorists believe that, despite the clear success of the Standard Model, there are compelling reasons to believe that it is none other than a very good low energy approximation to the ultimate theory. Another mass scale will be encountered at $\lesssim 1$ TeV. Some of the reasons cited are the gauge hierarchy problem (incredibly fine tuning is required to make the Standard Model work), the left-right asymmetry of the Standard Model, the presence of too many parameters, the absence of any understanding of the quark and lepton mass spectrum, the lack of understanding of the generation puzzle, etc.

2. History has taught us that experimental knowledge is always limited by the energy available at the last frontier crossed – new frontiers almost always bring with them new input. There are many instances of successful low energy approximations to the real world – Newtonian mechanics and the Fermi four-point theory of the Weak Interactions – to name but two.

3. Curiosity! No "self-respecting" experimentalist will accept the constraints of the current theories. Higher energy machines are the only way to know for sure what nature has in store – in the end, the **ultimate test** lies with the experimental data.

So these then are some of the reasons to push to the next frontier. We will first examine what we can learn from the Z^0 frontier ($E_{c.m.} = 93$ GeV). The Z^0 does not offer us a very substantial gain in energy relative to PETRA which has run at 44 GeV. However, as we will discuss, there are some special features of this Weak Interaction laboratory which give it an experimental reach far greater than the relatively small energy increase.

3. THE Z^0 MACHINES

To study most of the physics covered by these lectures we will require large numbers ($\gtrsim 10^5$) of Z^0 decays. We will also want to have an environment in which there is a minimal loss of decay channels arising from trigger and/or analysis techniques. The $\bar{p}p$ machines will provide valuable information about the Z^0, but the number of events will be sparse and all the Z^0 decay channels are not analyzable. As of now the UA1 and UA2 detector groups have less than 100 identified Z^0 events all of which are in the decay channel $Z^0 \to e^+e^-$ or $\mu^+\mu^-$. These two decay modes represent only about 6% of all Z^0 decays.

The high energy physics community is constructing two machines capable of providing $\simeq 10^6$ Z^0's per year. The LEP machine is under construction at CERN and the SLC machine is being built at SLAC. These two Z^0 "factories" are quite different machines and they offer different experimental possibilities. The LEP machine is a conventional e^+e^- storage ring – a scaled up version of PETRA at DESY and PEP at SLAC. It uses well-understood, proven technology and should perform close to its design specifications shortly after beam turn-on. The SLC (Stanford Linear Collider) uses an entirely new concept in accelerator technology and, in that sense, is a less certain path to high luminosity. However as we will see, the SLC is a pioneering effort in the area of linear colliders which provide the only affordable means to TeV e^+e^- colliding beam physics. The SLC will serve both as a prototype for future high energy colliding linacs and as a copious source of Z^0's. How do the two approaches differ?

3.1 CONVENTIONAL e^+e^- STORAGE RINGS

In a conventional e^+e^- storage ring one or more bunches of electrons and positrons are stored, travelling in opposite directions, in a magnetic guide field. Collisions occur at fixed points around the ring (so-called interaction regions) and there are $2n_b$ collision points possible where n_b is number of bunches. The particle detectors are placed in the interaction regions. The magnetic guide field comprises a) dipoles which provide the restoring force for a closed $e^\pm$ orbit b) quadrupoles for focussing the e^+ and e^- beams and c) sextuples to remove or reduce chromatic abberations in the magnetic focussing system.

Storage rings suffer substantial energy loss from synchrotron radiation. An electron of energy E_{beam}, travelling in a circle of radius R, loses an amount

$$\Delta E = 88.5 \times 10^{-6} \ (\text{meter GeV}^{-3}) \ \frac{E_{\text{beam}}^4}{R} \qquad (1)$$

of energy per revolution. An $e^\pm$ at PEP loses about 10 MeV/revolution for E_{beam} = 14.5 GeV. This power must be restored by RF cavities placed at strategic

points around the storage ring. At full current (40 mamps) the PEP machine requires 6 MW of RF power. It is important to notice the $E^4_{\rm beam}$ dependence in the synchrotron radiation loss – there is a substantial penalty paid as one raises the beam energy of a storage ring.

The rate for a process with cross section σ is

$$\text{rate} = \mathcal{L}\ \sigma$$

where $\mathcal{L}$ is the luminosity measured typically in units of $\text{cm}^{-2}\ \text{sec}^{-1}$. For the collision of an e^+ and e^- bunch, the luminosity is given by

$$\mathcal{L} = \frac{N^+ N^- f}{A} \tag{2}$$

where $N^\pm$ is the number of $e^\pm$/bunch, f is the collision frequency and A is the area of the larger of the two beams. Typical luminosities for existing storage rings are $\simeq 10^{31}\ \text{cm}^{-2}\ \text{sec}^{-1}$. The luminosity does not grow without bound; as one adds increasing amounts of $e^\pm$ to the beams, the continuous passage of one beam through the other causes one or both of the beams to grow, thereby reducing the luminosity. It is the cumulative effect of many small perturbations that causes the beam-beam interaction to limit the luminosity. In addition one can only tolerate as much beam current as one has RF power to suitably restore the energy lost to synchrotron radiation.

Typical beam sizes in a storage ring are

$$\sigma_x \approx 500\ \mu\text{m}$$

$$\sigma_y \simeq 50\ \mu\text{m}$$

and

$$\sigma_z \simeq 2\ \text{cm}$$

where x is the coordinate in the direction of the dipole magnet field (*i.e.* horizontal), y is vertical and z is measured along the beam direction. The beam size is limited by the synchrotron radiation damping and excitation, again a process resulting from the multiple revolution nature of the machine.

What limits the center of mass energy ($E_{\text{c.m.}} = 2E_{\rm beam}$) achievable with storage rings? It turns out that the economics of very high energy storage rings is very unfavorable. We can write the equation for the cost (C) of a storage ring as

$$C = \alpha R + \beta\ \frac{E^4_{\rm beam}}{R} \tag{3}$$

where α and β are constants and R is the radius of the machine. The first term in the cost equation arises from elements needed to build the ring – tunnels,

vacuum system, ring magnets etc. The second term comes from the RF system (see equation (1)). Let us suppose that we minimize the cost as a function of radius R. Differentiating and setting $dC/dR = 0$ one finds

$$R = (\beta/\alpha)^{1/2}\ E_{\text{beam}}^2$$

$$C = 2(\beta/\alpha)^{1/2}\ E_{\text{beam}}^2\ .$$

Hence the cost of the construction of a storage ring scales like E_{beam}^2 as does the radius (real estate). Lets look at some concrete examples starting with the LEP machine as a guide. The first phase of LEP will be a 50×50 GeV machine with conventional RF, circumference = 27 km and C = \$500 M. Suppose we scaled this up to a 500×500 GeV machine: circumference $\rightarrow$ 2700 km and $C \rightarrow$ \$50,000 M! Clearly such a machine is prohibitively expensive. Can one improve the situation by using superconducting RF? The second (superconducting) phase of LEP will be a 100×100 GeV machine at a cost of about \$700 M. Hence using superconducting RF our 500×500 GeV machine will have parameters circumference = 675 km and C = \$17,500 M – still far too costly! So clearly we need a different technology to pursue e^+e^- physics in the TeV energy range. This brings us to option 3.2.

3.2 The Linear e^+e^- Collider

In a linear collider machine one envisages two linear accelerators firing beams of electrons and positrons at each other. Following the collision, the beams are discarded. The detector is placed at the collision point. In such a machine the cost will scale like E_{beam}; $C = \alpha' E_{\text{beam}}$ and one gets away from the E_{beam}^2 scaling law of the storage ring. If one started building machines from scratch (no existing accelerator facilities) the constants α, β and α' are such that the cost of the linear collider and a storage ring are equal at roughly $E_{\text{c.m.}} \approx 150-200$ GeV. Above this energy range the linear collider becomes increasingly more economical. How does one achieve useful luminosities in a linear collider? The luminosity is given by equation (2). For LEP $f \approx 50{,}000$ while for a linac (SLAC) $f \approx 200$. Typically N^+N^- will be larger for the storage ring than for linear colliders, but not by much. The only way then to get a linear collider luminosity comparable to a storage ring is to reduce the beam size A in the collider by about 10^5 relative to the beam size in the storage ring. As discussed earlier the beam size in a storage ring is limited by the synchrotron radiation losses. The colliding linac does not suffer from this problem – the beam size is limited by the emittance of the linac beam. The emittance can be controlled to yield beam sizes on the order of 10 $(\mu\text{m})^2$. Hence, in principle, the reduction in frequency and bunch particle number density can be largely offset by the reduction in beam size and a colliding linac luminosity of $\approx 10^{31}$ should be possible.

The dynamics of the beam-beam interaction is very different in colliding linacs than in a storage ring. This problem is discussed fully in reference 3. The major difference comes about from the fact that the charge density in the colliding linacs is considerably (several orders of magnitude) higher than in a storage ring. The maximum current which can be collided in the colliding linac machine will still be limited by the beam-beam interaction. However the nature of the beam-beam interaction is very different in the colliding linac. The collision of the two high current density beams is very disruptive and tends to blow the beams apart. For sufficiently high currents (charge density) the passage of the one beam through the other causes a reduction (focusing) of beam size prior to the destructive disruption of the beams. This so-called "pinch" effect therefore enhances the luminosity in a linear collider system. Figure 1 (taken from reference 3) shows the pinch effect graphically. Four "snapshots" of the beam profiles in x, transverse to the beam, and z, along the beams, are shown. The upper two snapshots are taken as the e^+ and e^- beams approach each other. The third snapshot shows dramatically how the beam size has been squeezed down and in the forth the beams have passed "through" each other and are beginning to "explode." In a machine like the SLC, the "pinch" effect is expected to produce a factor of ~ 6 increase in luminosity. As stated before, linear colliders are an untested technology – the problems of producing and colliding micron size beams are by no means solved. However they will receive their first real test with the commissioning of the SLC.

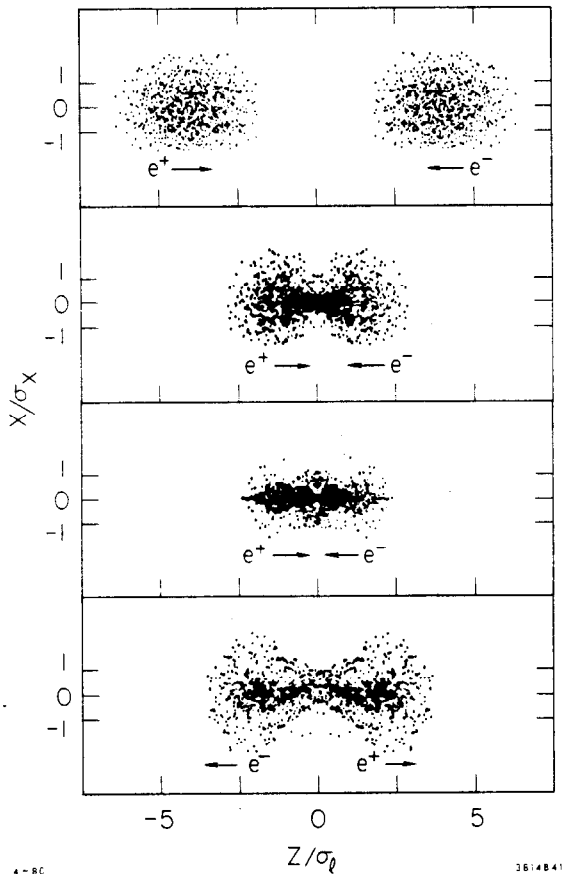

Fig. 1. Side view of the collision of oppositely charged beams showing the "pinch" effect. The coordinate z is measured along the beam direction, x is transverse to the beam direction.

3.3 THE LEP MACHINE

LEP will be a conventional e^+e^- storage ring and a comprehensive description can be found in reference 4. The ring is being built at CERN and will have a circumference of 27 km. In its first incarnation (LEPI) it will achieve a maximum collision energy of 100 GeV and a luminosity of 10^{31} cm^{-2} sec^{-1}. 16 MW of conventional RF will be required for LEPI and the machine is expected to deliver collisions in late 1988. The initial outlay for LEP will be \$500 M and it will have eight experimental halls – four of which will be instrumented at the beginning. The initial detectors go by the names of LEP3, OPAL, DELPHI and ALEPH. Typically these detectors will cost \$50 M to build.

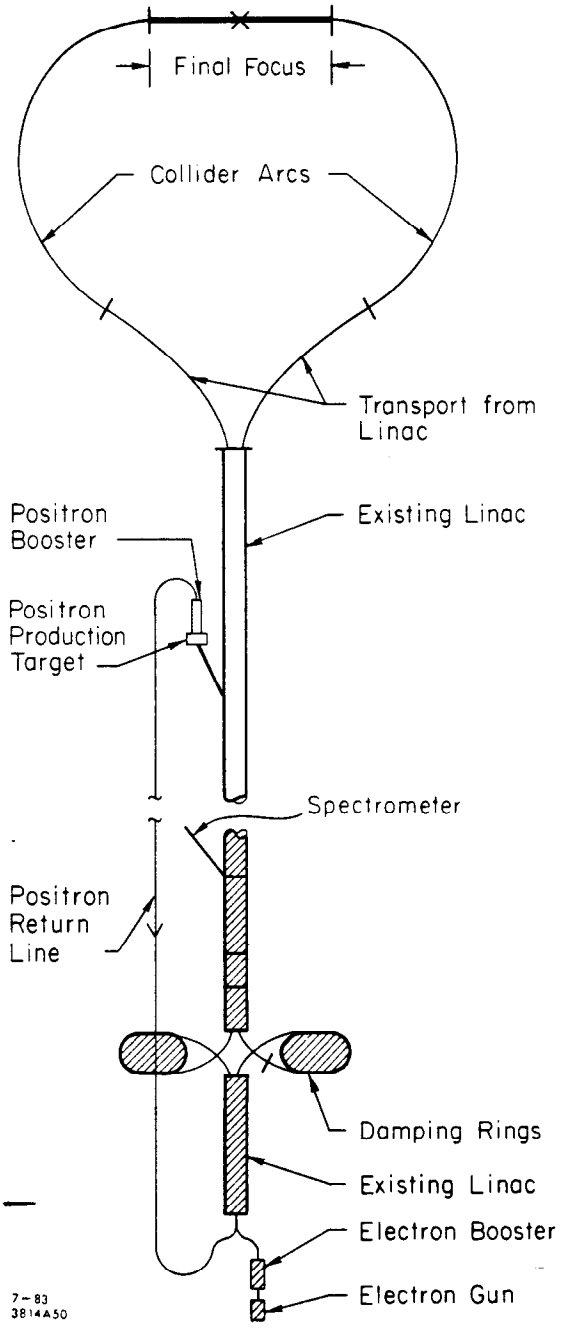

Fig. 2. Schematic of the SLC machine.

The LEPI machine will be upgraded to $E_{\text{c.m.}} \sim 170$ GeV by the addition of 80 MW of RF power and then to $E_{\text{c.m.}} \gtrsim 200$ GeV using superconducting RF cavities. The time scale for these upgrades is not yet known. Since the LEPI machine relies on conventional techniques, design performance should be reached soon after the first collisions.

3.4 THE SLC MACHINE

The SLC machine is being built at SLAC and is slated to deliver colliding beams at the Z^0 in late 1986. The design luminosity of the machine is 6×10^{30} cm^{-2} sec^{-1} and the maximum energy at turn-on will be 100 GeV. A complete description of the SLC can be found in reference 5. However, since the SLC is not a conventional e^+e^- storage ring, we provide here a short description of the machine referring to figure 2. The existing linac will be upgraded to

50 GeV using new high-powered klystrons. An electron bunch is diverted out of the linac and collided with a target to produce positrons. These positrons are then fed back into the front end of the accelerator. Following passage through damping rings, which provide cooling for the electron and positron bunches, a bunch of positrons immediately followed in the next linac bucket by a bunch of electrons, is transported down the accelerator to the colliding arcs. The positrons and electrons are switched to different arcs and are brought into collision by an elaborate system of optics, termed the final focus. Following the collision, the beams are dumped. So unlike a storage ring, the SLC operates as a single pass collider. The repetition rate of the linac is 180 Hz, many orders of magnitude less than that of typical storage rings. To produce a usable luminosity, this slow collision rate will be compensated for using an intense electron gun capable of producing 7×10^{10} electrons per bunch and by designing the final focus optics such that the transverse dimensions of the colliding beams are a few microns. The expected luminosity as a function of collision energy is shown in figure 3. The SLC is optimized to run at the Z^0 . However, the luminosity remains good down to $E_{c.m.} \approx 60$ GeV. If toponium is beyond the reach of the TRISTAN machine,[6] the SLC could be used to study toponium. The energy spread of the SLC machine will be about 0.2% at full luminosity and about 0.1% at a somewhat reduced luminosity. This can be compared with LEP which will have an energy spread of 0.1%.

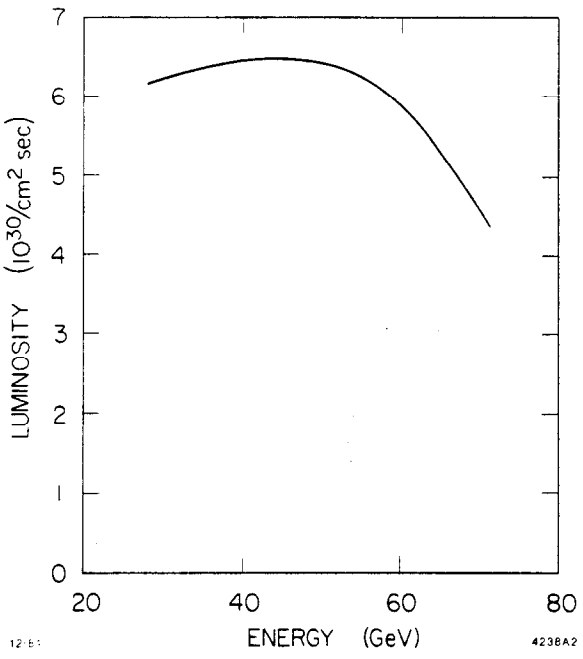

Fig. 3. The luminosity of the SLC as a function of E_{beam}.

Another feature of the SLC is the promise of longitudinally polarized beams, which, as we shall discuss, is a powerful tool for the study of Z^0 physics.[7] Polarized electrons are produced by shining circularly polarized laser light on a gallium arsinide cathode. Such an electron gun exists and has been successfully tested. Polarized electrons have already been transported down the linac and simulations of transport through the SLC arcs indicate that the transmission efficiency for the polarized electrons is $\geq$ 80%. The sign of the laser polarization can be reversed on a linac pulse-by-pulse basis yielding successive beam pulses of opposite polarizations. Hence it appears that, with very high

probability, beams with polarizations of $\geq 50\%$ will be available at the SLC. Beam polarization at LEP is much less certain. The problems of producing and retaining the longitudinal polarization are many and no good solutions exist at this time. (See reference 4, page 132.)

The SLC machine has the distinct disadvantage of having only one interaction region. Because of the newness of the technology, it will take a considerable time and machine physics effort to reach design luminosity. The first detector for the SLC will be an upgraded MARK II detector. This detector has had six months of testing at PEP and is being installed at the SLC. A LEP competitive detector, the SLD, is also being built. This detector is scheduled to begin physics running at the SLC in late 1989 and once it has been checked out it will replace the MARK II.

What about the event rate at the Z^0? As we will see later, the cross section running on the Z^0 is about 50 nb. However initial state radiation reduces this to a usable cross section of about 40 nb. Assuming an average luminosity of 1.5×10^{30} cm^{-2} sec^{-1}, one finds an event rate of 5200 Z^0/day! Assuming 200 days for physics one has an event rate of 10^6 Z^0/year. During these lectures we will use this as a benchmark for calculating rates. Realistically during its first full year, the SLC might achieve 10^5 Z^0's, corresponding to an average luminosity of 1.5×10^{29} cm^{-2} sec^{-1}.

4. THE STANDARD MODEL AND ITS APPLICATION TO $e^+e^- \rightarrow Z^0 \rightarrow f\bar{f}$

For most of these lectures we will assume the Standard Model. During the last lecture we will look beyond the Standard Model at which time we will develop whatever formalism we need. The goal of this section is not to be complete or detailed – but merely to build a foundation from which we can extract useful experimental tests at the Z^0 .

The Standard Model is characterized by the gauge group

$$SU(3)_{\text{color}} \wedge SU(2) \wedge U(1) \quad .$$

Leptons are pointlike particles which couple to the gauge bosons of $SU(2)$ through their weak charge and to the photon of $U(1)$ through their electric charge. There are six leptons e, μ, τ, and their zero mass partners ν_e, ν_μ, and ν_τ. There are six quarks u, d, s, c, b and t which carry color and there are three color states for each quark. Leptons have no color charge and are therefore "blind" to the strong interaction.

The left handed fermions are arranged in weak iso-doublets

$$\begin{pmatrix}\nu_e\\ e\end{pmatrix}_L \quad \begin{pmatrix}\nu_\mu\\ \mu\end{pmatrix}_L \quad \begin{pmatrix}\nu_\tau\\ \tau\end{pmatrix}_L \qquad \begin{matrix}T_3 = 1/2\\ -1/2\end{matrix}$$

$$\begin{pmatrix}u\\ d'\end{pmatrix}_L \quad \begin{pmatrix}c\\ s'\end{pmatrix}_L \quad \begin{pmatrix}t\\ b'\end{pmatrix}_L \qquad \begin{matrix}T_3 = 1/2\\ -1/2\end{matrix}$$

where T_3 is the 3rd component of the weak charge. The primes on the quarks indicate that flavor conservation in the quark sector is not perfect. This generation mixing can be summarized by the elements of the Kobayashi-Maskawa matrix – the most familiar component being the Cabibbo angle which tells us that the d quark has a $\sim 5\%$ strange quark admixture. More succinctly – in the quark sector the weak eigenstates are related by a rotation matrix to the mass eigenstates. There are no analogous flavor changing currents in the neutral sector. We notice in passing the peculiarity of the three generations, the ν_e, e, u and d' being the members of the lightest generation. The Standard Model does not explain why nature chooses to replicate itself in this peculiar manner.

Right handed fermions appear in singlets, u_R, d_R $\ldots t_R$, e_R, μ_R, τ_R and, since the ν's are massless, there are no right handed ν's. $T_3 = 0$ for all right handed fermions.

There are nine massless bosons in the Standard Model – 8 gluons and the photon. There are 3 massive vector bosons W^+, W^- and Z^0 and, in the minimal model with one Higgs doublet, there is one neutral scalar, H^0. Gluons carry color (unlike photons which don't carry charge) and hence $SU(3)_{\text{color}}$ is non-abelian. Since gluons carry color they can couple to other gluons. The polarization of the QCD vacuum by virtual quark and gluon pairs results in an anti-screening of color charge. This can be contrasted with the screening of electric charge by virtual e^+e^- pairs in QED. This anti-screening leads to the notion of confinement of quarks and the decrease of the strong coupling constant α_s, with increasing q^2. Free quarks should not be seen and this notion will be tested at the Z^0 although not discussed further in these lectures.

The Standard Model does not predict masses for the fundamental particles. The $W^\pm$, Z^0 masses are given in terms of the parameter $\sin^2\theta_W$:

$$M_W^2 = \frac{\pi\alpha}{\sqrt{2}G_F}\left(\frac{1}{\sin^2\theta_W}\right)$$

$$M_{Z^0}^2 = \frac{M_W^2}{\cos^2\theta_W} = \frac{\pi\alpha}{\sqrt{2}G_F}\left(\frac{1}{\sin^2\theta_W\cos^2\theta_W}\right)$$

where α is the fine structure constant and G_F is the Fermi coupling constant. The H^0 mass is expected to fall in the range $7.5 \lesssim M_{H^0} \lesssim 10^3$ GeV. This however

is of no consolation to the experimentalist searching for the H^0. The presence of the neutral Higgs is crucial to the success of the Standard Model.

The electroweak interactions of all the gauge fields are specified by the Model and are determined by e, the electric charge, and one free parameter θ_W. Spinors couple to the photon field with strength e and to the Z^0 with strength

$$-\frac{e}{\sin\theta_W\cos\theta_W}\left(T_3^{R/L}-Q\sin^2\theta_W\right)=2\sqrt{2}\left(\frac{M_Z^2G_F}{\sqrt{2}}\right)^{1/2}\left(T_3^{R/L}-Q\sin^2\theta_W\right)$$

where R/L indicates left and right couplings and Q is the charge of the fermion.

Aside from Higgs and fermion masses, the Electro-Weak theory is totally specified if we know α, G_F and M_Z. α and G_F are extremely accurately (better than one part in 10^5) known, M_Z is known only to about 3%. A precise measurement of M_Z will constrain considerably the Standard Model.

For almost all the physics discussed in these lectures, we are interested in the basic process $e^+e^-\to f\bar{f}$ where the symbol f signifies a fundamental fermion, either a quark or a lepton. There are two processes which contribute to the cross section as shown in figure 4, namely $e^+e^-\to\gamma\to f\bar{f}$ and $e^+e^-\to Z^0\to f\bar{f}$. The Standard Model specifies all the couplings and hence the cross section for these processes can be calculated. If θ is the fermion polar angle, the differential cross section has the form[8]

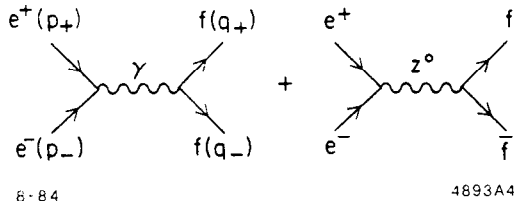

Fig. 4. The basic $e^+e^-\to\gamma,\ Z^0\to f\bar{f}$ process.

$$\begin{aligned}\frac{d\sigma_{f\bar{f}}}{d\cos\theta}=&\frac{\pi\alpha^2Q_f^2D}{2S}\left(1+\cos^2\theta\right)-\frac{\alpha Q_fDG_FM_z^2(S-M_z^2)}{8\sqrt{2}[(S-M_z^2)^2+M_z^2\Gamma_z^2]}\\&\left[(R_e+L_e)(R_f+L_f)(1+\cos^2\theta)+2(R_e-L_e)(R_f-L_f)\cos\theta\right]\\&+\frac{DG_F^2M_z^4S}{64\pi[(S-M_z^2)^2+M_z^2\Gamma_z^2]}\\&\left[(R_e^2+L_e^2)(R_f^2+L_f^2)(1+\cos^2\theta)+2(R_e^2-L_e^2)(R_f^2-L_f^2)\cos\theta\right]\end{aligned}\tag{4}$$

where Q_f is the fermion charge, $S=E_{c.m.}^2$, M_Z the mass of the Z^0 and D takes into account the number of color degrees of freedom. For $f\equiv$ quark, $D=3$, otherwise $D=1$. The left and right handed weak coupling constants are given

by

$$L_f = T_3^f - Q_f \sin^2\theta_W$$

$$R_f = -Q_f \sin^2\theta_W \quad .$$

The three terms in the cross section are the purely electromagnetic contribution, the interference between the weak and electromagnetic diagrams and the purely weak contribution. Notice that a) the interference term disappears at $\sqrt{S} = M_Z$ as it should b) the first term is just the point QED differential cross section and c) at $\sqrt{S} = M_Z$ the purely weak term dominates.

It is illustrative to integrate over $\cos\theta$ and plot the cross section as a function of $E_{c.m.} = \sqrt{S}$. This is shown in figure 5. One sees that below the region of the Z^0 mass the purely electromagnetic cross section dominates as is reflected by the $E_{c.m.}^{-2}$ behavior. On the Z^0 pole however the weak cross section dominates, providing 10^3 times more particle production than the electromagnetic process. This is part of the magic of running at the Z^0 – the Z^0 provides an enormous enhancement in event rate over running in the continuum (*i.e.* off resonance). Studying e^+e^- interactions at ~ 93 GeV in the absence of the Z^0 with the SLC or LEP ($\mathcal{L}_{\text{peak}} \sim 5 \times 10^{30}$) would be extremely painful if not in many cases impossible. The presence of the Z^0 however renders these relatively low luminosity machines capable of very high event rates.

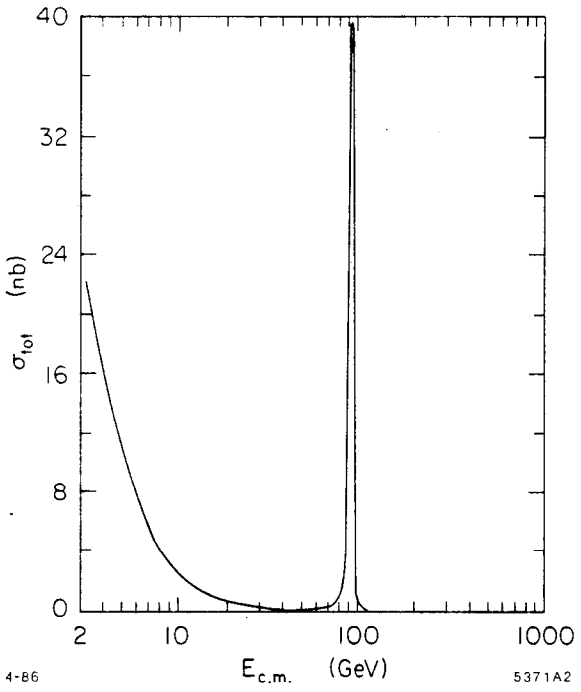

Fig. 5. The cross section for $e^+e^- \to \gamma, Z^0 \to f\bar{f}$ as calculated in the Standard Model. The $c\bar{c}$ and $b\bar{b}$ threshold behavior are omitted from the plot.

Let us now return to $d\sigma/d\cos\theta$ and consider running at $S = M_Z^2$, namely on the Z^0 pole. Changing notation to axial and vector coupling constants

$$a = \frac{1}{2}(L - R) \quad \text{and} \quad v = \frac{1}{2}(L + R)$$

one finds $L = a + v$, $R = v - a$, $L^2 + R^2 = 2(a^2 + v^2)$, $L^2 - R^2 = 4av$ and

$$\frac{d\sigma_{f\bar{f}}}{d\cos\theta} = \frac{DG_F^2 M_Z^4}{16\pi\Gamma_Z^2}\left[(a_e^2 + v_e^2)(a_f^2 + v_f^2)(1 + \cos^2\theta) + 8a_e v_e a_f v_f \cos\theta\right] \quad . \qquad (5)$$

It is useful to tabulate the couplings and the sum of their squares. Assuming $\sin^2\theta_W = 0.22$ (which we will do throughout for convenience) we find the values in table I.

TABLE I

	Q	T_3	a	v	$a^2 + v^2$
e, μ, τ	-1	$-1/2$	$-1/2$	$-.06$	.2536
ν_e, ν_μ, ν_τ	0	1/2	1/2	1/2	1/2
d, s, b	-1/3	$-1/2$	$-1/2$	$-.35$	.375
u, c, t	+2/3	+1/2	1/2	.21	.29

We turn our attention back to equation (5). The term linear in $\cos\theta$ contributes a front-back asymmetry, A_{F-B}. $A_{F-B} \propto v_e v_f$ which, for charged leptons, is a very small number. However a measurement of A_{F-B} for charged leptons has great sensitivity to $\sin^2\theta$ as we will see later in this section. Since $\int_0^\pi \cos\theta d\theta = 0$ the term linear in $\cos\theta$ does not contribute to the total cross section.

Integrating the term in $(1+\cos^2\theta)$ yields the total cross section for producing a final state $f\bar{f}$ at the Z^0 :

$$\sigma_{f\bar{f}} = \frac{DG_F^2 M_Z^4}{6\pi\Gamma_Z^2}\,(v_e^2 + a_e^2)(v_f^2 + a_f^2) \; .$$

We omit here the derivation of Γ_Z but note that

$$\Gamma_Z = \frac{G_F M_Z^3}{24\sqrt{2}\pi}\sum_i (v_i^2 + a_i^2) D_i \qquad (6)$$

where i ranges over all fundamental fermions and D_i is the color factor (3 for quarks, 1 for leptons). We can obtain σ_{point}, which is the lepton point QED cross

section, from the first term in equation (4):

$$\sigma_{\text{point}} = \frac{\pi\alpha^2}{2S}\int (1+\cos^2\theta)\; d\cos\theta$$

$$= \frac{4\pi\alpha^2}{3S} \simeq \frac{87\text{ nb}}{S}\ .$$

Hence we can write

$$R_{f\bar{f}} = \frac{\sigma_{f\bar{f}}}{\sigma_{\text{point}}} = \frac{D(a_f^2+v_f^2)(a_e^2+v_e^2)}{16\alpha^2(1-2x_W+8x_W^2/3)^2}\ . \tag{7}$$

Assuming 6 quarks, ignoring the finite t mass and setting $x_W = \sin^2\theta_W = .22$, one finds at the Z^0 the R values in table II. Also shown in table II are the branching fraction for each process. Hence under these assumptions $R_{Z^0} \approx 5200$ and $B(Z^0 \to \text{hadrons}) \simeq 72\%$. This value of R_{Z^0} has not been corrected for initial state radiation effects which has the effect of lowering the peak cross section with a compensating "radiative tail" on the high side of the resonance. These radiative effects are discussed more fully in reference 9 – we quote here the approximate result. For a narrow resonance with peak cross section σ_0 the actual cross section, after the inclusion of radiative effects, is

$$\sigma_{\text{peak}} \approx \left(\frac{\Gamma}{m}\right)^t \sigma_0 + \left(\delta_0 + \frac{13}{2}t\right)\sigma_0$$

TABLE II

CHANNEL $(f\bar{f})$	$R_{f\bar{f}}$	$\Gamma_{f\bar{f}}/\Gamma_{Z^0}$ (%)
each $\nu\bar{\nu}$	313	6.1
$\mu^+\mu^-$, $\tau^+\tau^-$, e^+e^{-*}	159	3.1
$u\bar{u}$, $c\bar{c}$, $t\bar{t}$	550	10.6
$d\bar{d}$, $s\bar{s}$, $b\bar{b}$	704	13.6

* We have ignored t channel diagrams which are only important at small values of θ.

where $t = 2\alpha/\pi\ (\ell n\ S/m_e^2 - 1)$ is the so called equivalent radiator and $\delta_0 = 2\alpha/\pi\ (\pi^2/6 - 17/36) \simeq 0.005$. At $\sqrt{S} = M_Z$, $t = .11$ and

$$\sigma_{\text{peak}} \approx 0.8\sigma_\sigma\ .$$

Hence the radiatively corrected R is approximately 4200 on the Z^0 .

We return now to the problem of how to incorporate the effects of large masses ($\omega rt\ \sqrt{S}$) for the final state fermion in equation (4). In a general way we can write

$$\frac{d\sigma_{f\bar{f}}}{d\theta} = f(\beta_f, \theta)\ \sigma(m_f = 0)$$

and

$$\sigma_{f\bar{f}} = f(\beta_f)\sigma(m_f = 0)$$

where β_f is the fermion velocity and m_f is the fermion mass. For <u>vector</u> couplings

$$f(\beta_f, \theta) = \frac{3}{16\pi}\ \beta_f[(1 + \cos^2\theta) + (1 - \beta_f^2)\sin^2\theta]$$

and

$$f(\beta_f) = \frac{1}{2}\ \beta_f(3 - \beta_f^2)\ .$$

For <u>axial-vector</u> couplings

$$f(\beta_f, \theta) = \frac{3}{16\pi}\ \beta_f^3(1 + \cos^2\theta)$$

and

$$f(\beta_f) = \beta_f^3\ .$$

Therefore for the t quark with velocity β_t, the correct form of the contribution to the Z^0 width is (see equation (6))

$$\Gamma(Z^0 \to t\bar{t}) = \frac{G_F M_Z^3}{8\sqrt{2}\pi}\left(v_t^2\ \frac{1}{2}\ \beta_t(3 - \beta_t^2) + a_t^2\beta_t^3\right)\ .$$

Figure 6 shows the suppression of $t\bar{t}$ relative to a full strength (light) charge two-thirds quark as a function of the t quark mass. Since we know from PETRA that $M_t \gtrsim 23$ GeV/c^2 the $t\bar{t}$ final state at the Z^0 is suppressed at least to 0.7 of the $u\bar{u}$ rate.

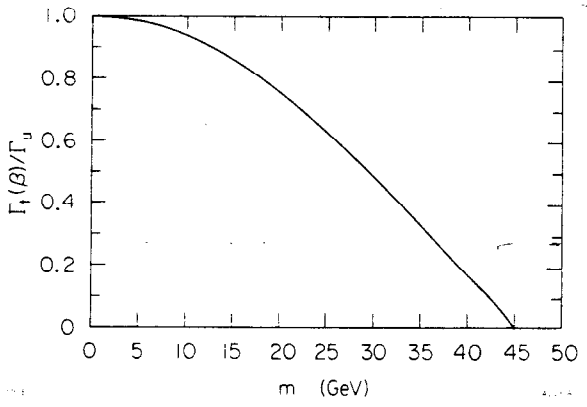

Fig. 6. The suppression factor of $t\bar{t}$ decays of the Z^0 as a function of M_t.

We return now to the forward backward charge asymmetry (A_{F-B}) discussed earlier. Consider for the moment the concrete example of the final state $\mu^+\mu^-$ as applied to our master formula (4). We will get a contribution to A^{μ}_{F-B} from terms linear in $z = \cos\theta$.

$$A^{\mu}_{F-B} = \frac{\int_0^1 \frac{d\sigma}{dz}dz - \int_{-1}^0 \frac{d\sigma}{dz}dz}{\int_0^1 \frac{d\sigma}{dz}dz + \int_{-1}^0 \frac{d\sigma}{dz}dz} = \frac{N^F_{\mu^-} - N^B_{\mu^-}}{N^F_{\mu^-} + N^B_{\mu^-}}$$

where $N^F_{\mu^-}(N^B_{\mu^-})$ is the number of μ^- in the forward (backward) hemisphere relative to the incoming e^- direction. On the Z^0 pole

$$A^{\mu}_{F-B} = \frac{3a_e a_\mu v_e v_\mu}{(v_e^2 + a_e^2)(v_\mu^2 + a_\mu^2)} \simeq 4.3\% \qquad (8)$$

for $\sin^2\theta_W = 0.22$. A^{μ}_{F-B} is proportional to $v_e v_\mu$ which makes it small, but very sensitive to $\sin^2\theta_W$. Rewriting the couplings in terms of $\sin^2\theta_W$ we find at the Z^0

$$A^{\mu}_{F-B} = \frac{3(1-4x_W)^2}{4(1-4x_W+8x_W^2)^2}\ , \quad x_W = \sin^2\theta_W$$

and

$$\frac{1}{15}\ \frac{dA^{\mu}_{F-B}}{A^{\mu}_{F-B}} \simeq \frac{d\sin^2\theta}{\sin^2\theta}\ . \qquad (9)$$

Hence the statement that a measurement of A^{μ}_{F-B} provides substantial sensitivity to $\sin^2\theta_W$.

From equations (7) and (8) applied to $e^+e^- \rightarrow Z^0 \rightarrow e^+e^-$ one finds

$$A^e_{F-B} = \frac{3a_e^2 v_e^2}{(a_e^2 + v_e^2)^2}$$

and

$$R^{e^-e^+} \propto (v_e^2 + a_e^2)^2 \ .$$

From these two equations one can determine a_e and v_e but not their relative sign. Is it possible to measure the relative sign? The answer is yes, as long as one can measure the fermion polarization of one of the charged $f\bar{f}$ final states. It turns out that the only practical final state for a polarization measurement is $\tau^+\tau^-$. Since parity is violated in the neutral current interaction, even in the absence of $e^\pm$ beam polarization, the Z^0 is produced polarized as are its decay products. The polarization P is given by

$$P^{f\bar{f}} = \frac{\sigma_R - \sigma_L}{\sigma_R + \sigma_L} = \frac{R_f^2 - L_f^2}{R_L^2 + L_f^2} = -\frac{2a_f v_f}{(a_f^2 + v_f^2)} \ .$$

Now the ratio

$$A^f_{F-B}/P^{f\bar{f}} = -3a_e v_e/(a_e^2 + v_e^2)$$

is independent of the final state fermion couplings and measures directly the relative sign of v_e and a_e. By measuring $R^{e^+e^-}$, A^e_{F-B} and the τ polarization one finds a_e and v_e and their relative sign. Then from $R^{\mu^+\mu^-}$, A^μ_{F-B}, $R^{\tau^+\tau^-}$, A^τ_{F-B} one can obtain the μ and τ axial and vector couplings. In this way the universality of the weak interactions is checked. In addition each measurement of a vector coupling provides a measurement of $\sin^2\theta_W$.

There remains one important issue which I have avoided but which is important to raise at this juncture. We have calculated the cross section for $e^+e^- \rightarrow Z^0 \rightarrow f\bar{f}$ in lowest order. However there are important weak radiative effects arising from one-loop diagrams such as are shown in figure 7. In order to compare the measurements at the Z^0 with the Standard Model, we must take these effects into account. To give you a feeling for their magnitude, inclusion of these one-loop diagrams changes (raises) the Z^0 mass by about $3\frac{1}{2}\%$. Happily these effects have been calcualted by several authors[10] and there is good agreement on their size. The exact

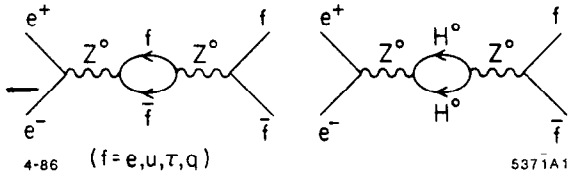

Fig. 7. One-loop weak radiative corrections to the process $e^+e^- \rightarrow Z^0 \rightarrow f\bar{f}$.

impact of those effects on an experimental measurement will depend crucially on the cuts which are applied to the data. Hence application of a Monte Carlo simulation, as opposed to analytical calculations, is the most reasonable way to extract the physics. Such Monte Carlo programs – with both weak and electromagnetic radiative effects – are being developed for both SLC and LEP. In addition, as we will see later, we will be able to check the validity of the radiative correction calculations from measurements made at the Z^0.

5. THE Z^0 ENVIRONMENT – REQUIREMENTS FOR DETECTORS

So it seems we will have two fine Z^0 "factories" – what kind of detectors do we need? The Z^0 environment has been studied in many workshops and the interested reader can find summaries of these workshops in references 11, 4 and 2. We describe here the main features of the environment, particularly as they pertain to detector design. The basic production process is shown in figure 8 where the final state particle naming convention is given in the figure caption. We now consider how these produced states decay. The final states e^+e^- , $\mu^+\mu^-$ are stable and result in opposite sign, high energy ($\sim E_b$) back-to-back leptons. The typical decays of the other produced states are shown schematically in figure 9. A quick glance at figure 9 and one realizes that what is needed at the Z^0 is a detector capable of a) measuring the properties of high energy jets b) measuring and tagging electrons and muons over a wide range of momenta both in isolation and in the presence of high energy jets and c) measuring the total energy and momentum in the event as an indicator of the missing energy and transverse momentum of ν's.

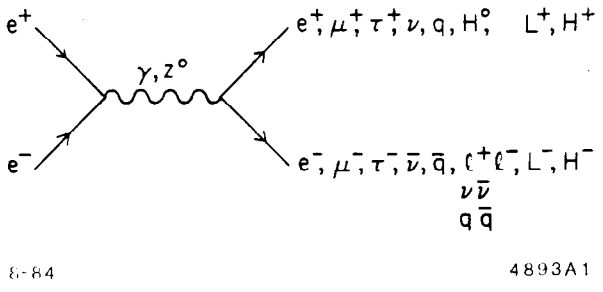

Fig. 8. The basic e^+e^- process where final states are produced via an intermediate photon or Z^0. The notation is obvious except that q stands for a quark, H^0 the neutral Higgs scalar, $\ell^\pm$ a charged lepton, $H^\pm$ a charged Higgs scalar and $L^\pm$ a (new) heavy charged lepton.

In addition there are many multi-jet and multi-lepton events which demands that the detector be uniformly instrumented over as large a solid angle as possible. Figure 10 shows the fractional momentum carried by hadrons, leptons and photons in events of the type $Z^0 \rightarrow$ hadrons. Notice the large dynamic range of the particle momenta. The detector must do an equally good job at high and low momenta. The high momentum (leading) particles carry information

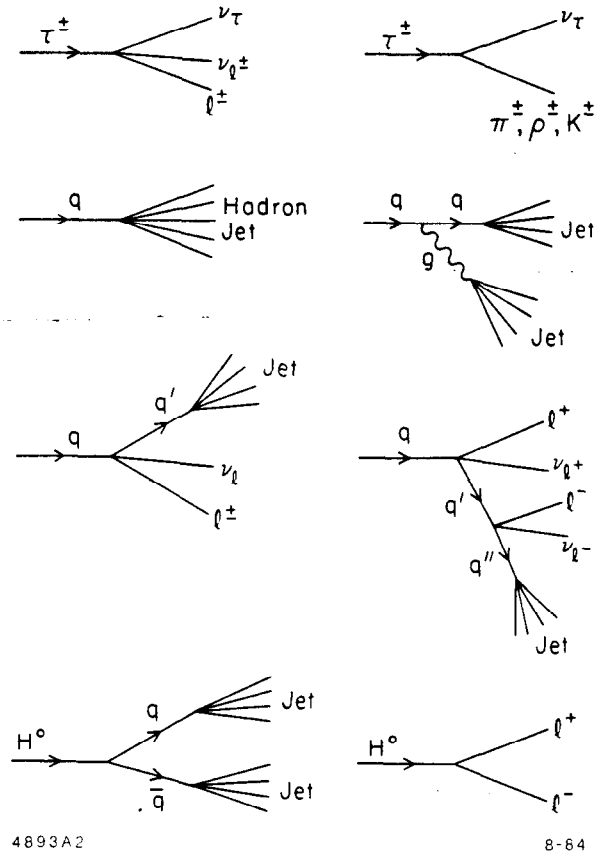

Fig. 9. Typical decays which result from the process in figure 4. The symbol g stands for a gluon, ℓ for lepton.

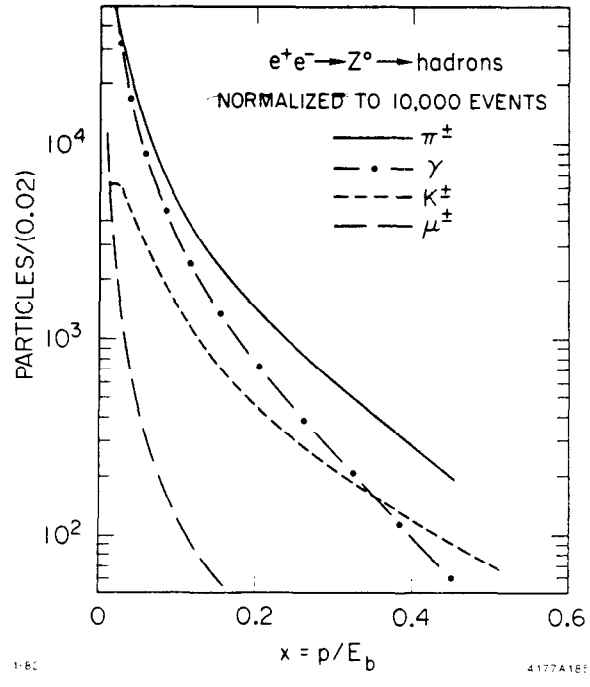

Fig. 10. Momentum distribution for different particle species produced in the decay of $Z^0 \rightarrow$ hadrons.

about the quark flavor and the fragmentation process, while the intermediate and low energy particles provide information about the decay chains and the energy flow. Typical multiplicities for the $Z^0 \rightarrow$ hadrons are 22 charged particles and 23 photons per event – jet multiplicities on the order of 11 charged particles and 11 photons. In addition this multiplicity is highly collimated – most jets are contained in a $\lesssim 10°$ cone. Figure 11 shows the angle between various particle species and the event jet axis. The distribution peaks at $\sim 2°$ for photons and hadrons. Hence a detector will have to possess fine segmentation both in the charged tracking and the calorimetry.

Studies[11] of reconstruction of K^0_S, D^0, $D^{\pm}$, measurement of the invariant cross section $Sd\sigma/dx$ (at high x), measurement of the $\tau^{\pm}$ polarization lead to the conclusion that a momentum resolution of $\sigma_p/p \lesssim 0.3\ P$ (GeV/c) is needed. In order to separate leptons from hadrons cleanly will require rejection of hadrons at a level of $\geq 10^3$. This can be understood in simple terms as follows. The average charge multiplicity is 10/jet and the typical semi–leptonic branching fraction

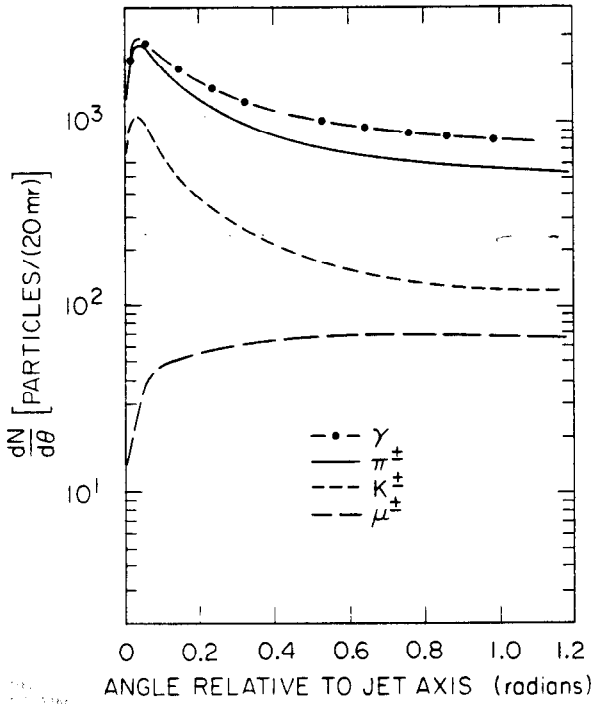

Fig. 11. Distribution of the angle with respect to the jet axis for different particle species in $Z^0 \rightarrow$ hadron events.

$(B(q \rightarrow \ell^{\pm}\nu x))$ is 10%. Hence in hadronic events one will have, on average, one $e^{\pm}$, $\mu^{\pm}$ per 100 charged hadrons. Having a signal to noise of 10 $e^{\pm}$, $\mu^{\pm}$ per 1 hadron requires a rejection of hadrons at the 10^3 level. A final requirement for a good detector in the new energy regime of the Z^0, is the ability to search for free quarks. This can be done by a) measuring the ionization of charged particles in a gas chamber (dE/dx) which measures charge directly or by b) using time of flight to look for massive particles.

It seems possible to design 4π detectors which are equal to most of the rigors of the environment described here. Although diverse in their approaches to the problems, the four LEP detectors and the SLD should do an excellent job of studying the Z^0 physics. The MARK II upgrade is a more modest approach designed to be ready for the early start of the SLC. Its main drawback is its lack of hadron calorimetry and hadronic particle identification. However as a survey detector, it will do most physics very well. For completeness a list of the detector proposals is given in reference 12 and a schematic of the upgraded MARK II detector is given in figure 12.

6. TESTING THE STANDARD MODEL AT THE Z^0

6.1 Measurements of the Z^0 Mass and Width

We recall from section 4 that, with the exception of particle masses, the Electro-Weak sector of the Standard Model is entirely specified by knowing α, G_F and M_Z. α and G_F are known very precisely[13] (to better than 1 part in 10^5) and presumably then the first task at the SLC and LEP will be to make a precise measurement of M_Z. To date, the best measurement of M_Z is provided by the UA2 group[14] of $M_Z = (93.5 \pm 2.5 \pm 1.3)$ GeV.

To measure M_Z requires mapping out the resonance shape by running the machine at discrete energy settings in the neighborhood of 93 GeV. The MARK II group[15] has made a study of optimum strategies for such an energy scan. Variables used to differentiate different scans are the number of scan points, the energy step and the amount of data logged at each point. Several optimum strategies were found; an example of one has 9 scan points, each 750 MeV apart and requiring 100 nb^{-1} or 3000 equivalent Z^0 events. Even at a low average luminosity of 2×10^{28} cm^{-2} sec^{-1}, this would only take two calender months. Based on statistics alone, such a scan would yield the following errors:

$$\delta M_Z = 45 \text{ MeV/c}^2 \ , \quad \delta \Gamma_Z = 135 \text{ MeV} \quad \text{and} \quad \delta R_Z = 3.5\% \ .$$

These numbers are impressive, especially the error on the mass. What would the systematics in the mass measurement be? Initial state radiation will shift the Z^0 mass peak down by about 250 MeV/c^2 – however this can be accurately calculated to within about 10 MeV/c^2. Energy dependent errors in the luminosity monitor measurement will change the line shape. However typical errors of this type (2%) would lead to small (10 MeV/c^2) errors in the mass determination. There are other effects; however the dominant effect will be the knowledge of the e^+ and e^- beam energies. Recognizing the potential limitation, two energy measuring spectrometers have been designed[15] for the SLC e^+ and e^- beam dump areas which will be capable of measuring $E_{c.m.}$ to 0.05%. This translates into a systematic uncertainty of 45 MeV/c^2 in M_Z. For normalization $\delta M_Z = 35$ MeV/c^2 corresponds to an error in $\sin^2\theta_W$ of 0.0002!

So it appears that with relatively little running, a few months at a very modest SLC luminosity, M_Z will be very accurately determined. Now if we believe the one-loop radiative correction calculations discussed in section 4, then we can input this accurate measurement of M_Z into the Monte Carlo simulation model and all Electro-Weak measurables and distributions should be very accurately predicted. (There will be effects arising from the unknown top and neutral Higgs masses. These will be discussed later – for almost all subsequent discussions

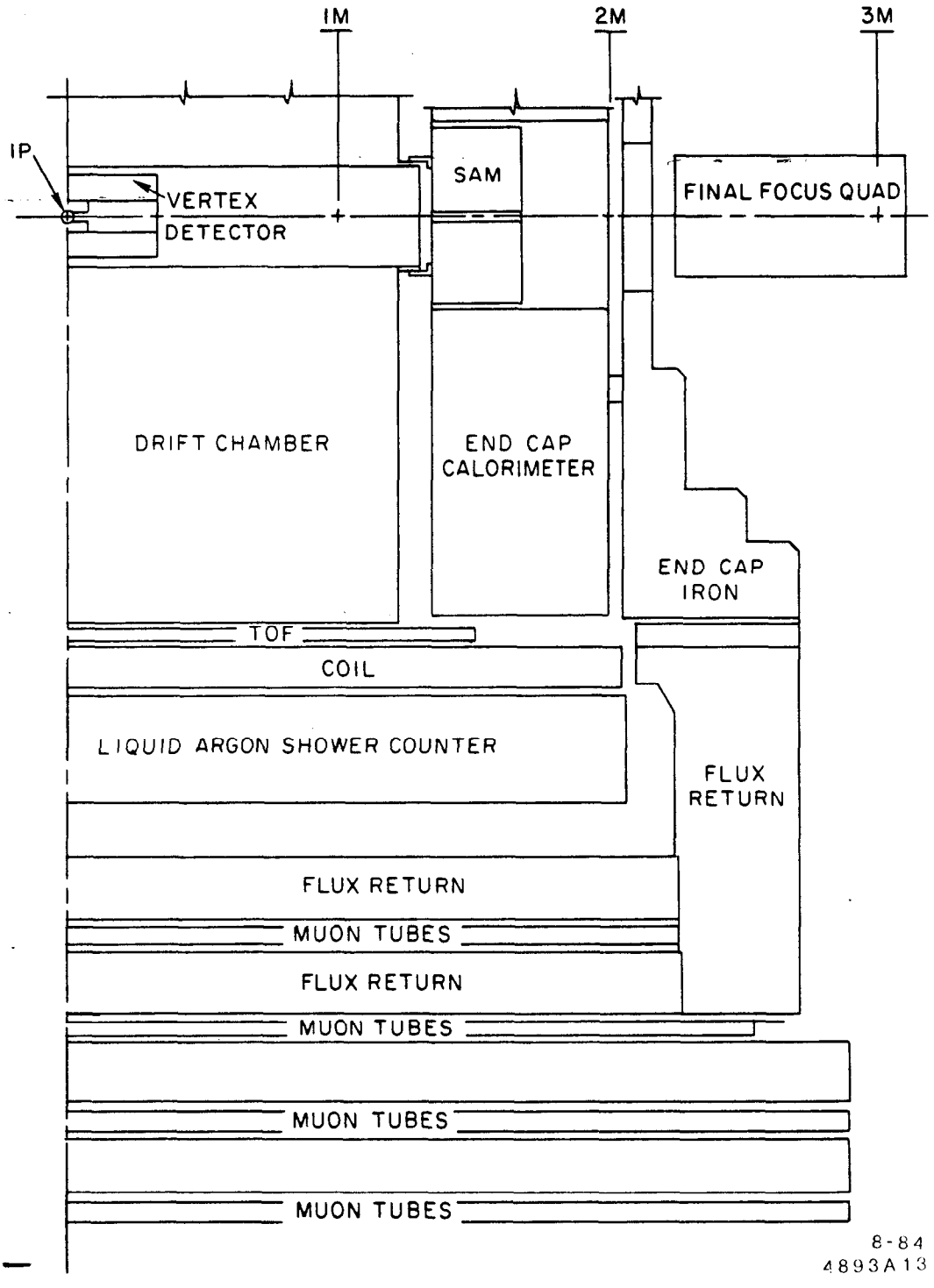

Fig. 12. A schematic of the Upgraded MARK II detector.

these can safely be ignored.) In particular we can use the Monte Carlo to predict the Z^0 line shape. How do the predicted width and peak cross section agree with data? New physics (including here the t quark) will change both of these quantities from the model predictions. Table III summarizes the changes in Γ_Z for various hypotheses. The combined measurements of Γ_Z and R_Z provided by the scan would have sensitivity to the presence of several of these alternatives. The exact nature of the anomalous width and cross section would not be revealed of course; we consider later how each one of those alternatives and others can be distinguished by looking at the event topologies.

TABLE III

Channel	Change in Γ_Z MeV
$\nu\bar{\nu}$	160
L^+L^-, $M_L = 30$ GeV/c^2	36
$q\bar{q}$, $M_q = 30$ GeV/C^2, $Q = -1/3$	211
$q\bar{q}$, $M_q = 40$ GeV/C^2, $Q = -1/3$	109
$q\bar{q}$, $M_q = 30$ GeV/C^2, $Q = 2/3$	144

Another way to measure Γ_Z is to recall from section 4 that for any $f\bar{f}$ final state:

$$\sigma_{f\bar{f}} = \frac{DG_F^2 M_Z^4}{6\pi \Gamma_Z^2} \left(v_e^2 + a_e^2\right)\left(v_f^2 + a_f^2\right) \quad .$$

Hence for each $f\bar{f}$ state one gets

$$\frac{d\Gamma_Z}{\Gamma_Z} = \frac{1}{2}\frac{d\sigma_{f\bar{f}}}{\sigma_{f\bar{f}}} \quad .$$

Given an accurate measurement of M_Z, the major experimental uncertainty will come from the luminosity measurement which can safely be done to $< 5\%$. This would yield an error $\delta\Gamma_Z < 70$ MeV per $f\bar{f}$ species. With a sample of 20,000 Z^0's the statistical error of both $\mu^+\mu^-$ and e^+e^- would be significantly less than that coming from the luminosity and, by adding these two channels, a 50 MeV measurement of the width would be possible. Referring again to table III, this would be a powerful indicator of new physics!

In summary then, with relatively little data, one can measure Γ_Z in two independent ways each one of which will yield an error ~ 50 MeV, these errors each being significantly smaller than the contribution of one ν species.

6.2 CHARGED LEPTON FINAL STATES

We now turn our attention to what can be learnt from specific topologies. Much can be learnt from studying the charged lepton final states. To do this we must isolate events of the type $Z^0 \to e^+e^-$, $\mu^+\mu^-$ and $\tau^+\tau^-$. This is a rather simple experimental task and is routinely done at PEP and PETRA. The experimental problems are even easier at the Z^0. For the e^+e^- and $\mu^+\mu^-$ final states one requires two opposite sign, charged particles which are "back-to-back" and carry the full beam energy. Electrons are trivially distinguished from muons using a rudimentary electromagnetic shower counter. To measure that the tracks have opposite sign requires only a modest momentum precision of $\sigma_p/p^2 \approx 1\%$ – all the LEP and SLC detectors will do far better than this. These channels have high rates ($B(Z^0 \to \ell^+\ell^-) = 3\%$) and there are no background problems. To identify the $\tau^+\tau^-$ final state one will probably require a topology in which the one τ decays to a single charged prong ($B(\tau \to 1$ charged prong $= 84\%)$) and the other τ decays to three charged prongs and any number of neutrals ($B(\tau \to 3$ charged prongs $= 16\%)$). This gives a very clean $\tau^+\tau^-$ sample at a rate of $3\% \times(2 \times 0.84 \times 0.16) \approx 1\%$. Hence the $\tau^+\tau^-$ final state will contribute information with a statistical weight of $\approx \sqrt{3}$ less than $\mu^+\mu^-$ or e^+e^- .

Consider now our canonical 10^6 produced Z^0's which will provide 30,000 $\mu^+\mu^-$ events. The asymmetry measurement will suffer a statistical error of $(\sqrt{30,000})^{-1} \simeq .005$. Hence (see equations (8) and (9))

$$\frac{\delta A}{A} = \frac{.005}{.043} = .12$$

and

$$\frac{\delta(\sin^2\theta)}{\sin^2\theta} = \frac{1}{15}\,(.12) = .008 \quad .$$

Assuming $\sin^2\theta_W = 0.22$, $\delta(\sin^2\theta_W) = .0017$! (Notice this is about an order of magnitude better than measurements from ν interactions or the polarized e^-d experiment.) The measurement error for the coupling constants is obtained after laborious propagation of errors which we omit here but are found in reference 11b page 28:

$$\delta(v/a) \simeq 0.008 \quad \text{for} \quad e^+e^-,\ \mu^+\mu^- \quad .$$

The measurements for the $\tau^+\tau^-$ channel will be less precise by about $\sqrt{3}$ as discussed above.

Notice now that we have a measurement of M_Z $(\sin^2\theta_W)$ and at least two more measurements of $\sin^2\theta_W$. Hence we are able to check the validity of the weak radiative correction calculations which, until now, we have assumed to be correct. Their effect was to modify $\sin^2\theta_W$ by 7%.

The measurement of R^{ee}, $R^{\mu\mu}$ and $R^{\tau\tau}$ amounts to counting the number of events in each category, making a correction for inefficiencies and normalizing to the luminosity. Typically these measurements can be done to $\lesssim 5\%$, the main limitation arising from the normalization. As we mentioned earlier, the final ingredient needed to measure the couplings is the measurement of the τ polarization. This is best done using the decay $\tau \to \pi\nu$, although the leptonic decays $\tau \to e\nu\nu$ and $\tau \to \mu\nu\nu$ are also useful. With modest particle identification the different τ modes can be identified. The measurable sensitive to the τ polarization is the $\pi^{\pm}$ or $\ell^{\pm}$ momentum spectrum. For a τ of polarization P_τ the fractional momentum of the π in the decay $\tau \to \pi\nu$ is given by[16]

$$\frac{dN_\pi}{dx_\pi} = 1 + P_\tau(2x_\pi - 1)$$

where $x_\pi = 2E_\pi/E_{c.m.}$. The average value of x_π is

$$\langle x_\pi \rangle = (3 + P_\tau)/6$$

and hence a measurement of $\langle x_\pi \rangle$ yields P_τ. Likewise[16] for $\tau \to \ell\nu\bar{\nu}$.

$$\frac{dN_\ell}{dx_\ell} = \frac{1}{3}\ \left[5 - 9x_\ell^2 + 4x_\ell^3 + P_\tau(1 - 9x_\ell^2 + 8_\ell^3)\right]$$

and

$$\langle x_\ell \rangle = (7 - P_\tau)/20\ .$$

So for the $\tau \to \pi\nu$ measurement we can select two prong and four prong events as shown in figure 13. One must now ensure that the single π's are indeed π's. This involves making sure that the track is neither a muon nor an electron. The separation of pions from muons and electrons in such a low multiplicity environment is easy particularly for momenta above 1 GeV/c. All the LEP and SLC detectors will be able to make a good separation. In addition making a good determination of $\langle x \rangle$ requires a momentum precision of $d\sigma_p/p^2 \lesssim 0.5\%$. The experimental details of the measurement are discussed in detail in reference 11b page 103 and we will borrow liberally from that discussion. We should remind ourselves that $P_\tau = -2a_\tau v_\tau/(a_\tau^2 + v_\tau^2) = f(\sin^2\theta_W)$ so

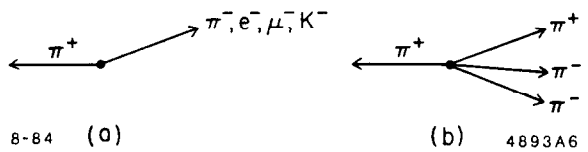

Fig. 13. Event topologies which could be used to study the decay $\tau^{\pm} \to \pi^{\pm}\nu_\tau$ via the production process $Z^0 \to \tau^+\tau^-$. In (a) the τ^- decays to a single charged prong, whereas in (b) the τ^- is envisaged as decaying to three charged pions.

that a measurement of P_τ is also a measurement of $\sin^2\theta_W$. In particular if $\sin^2\theta_W = 1/4$, $P_\tau \equiv 0$. Figure 14 shows the predicted dN/dx spectra for different values of $\sin^2\theta_W$. The simulation discussed in reference 11b used 10^6 Z^0's and a detector with parameters similar to the typical SLC/LEP detector. Figure 15 shows the simulated experimental momentum spectra for the decay pion and lepton where $\sin^2\theta_W$ has been set to 0.23. From these spectra the average values obtained are

$$\langle x_\pi \rangle = 0.483 \pm 0.006$$

$$\langle x_\ell \rangle = 0.359 \pm 0.003 \quad .$$

The solid lines on the figure correspond to the theoretical curves from figure 14 and demonstrate how the finite momentum resolution ($\sigma_p/p^2 = 0.5\%$ for this simulation) distorts the high x end of the spectrum.

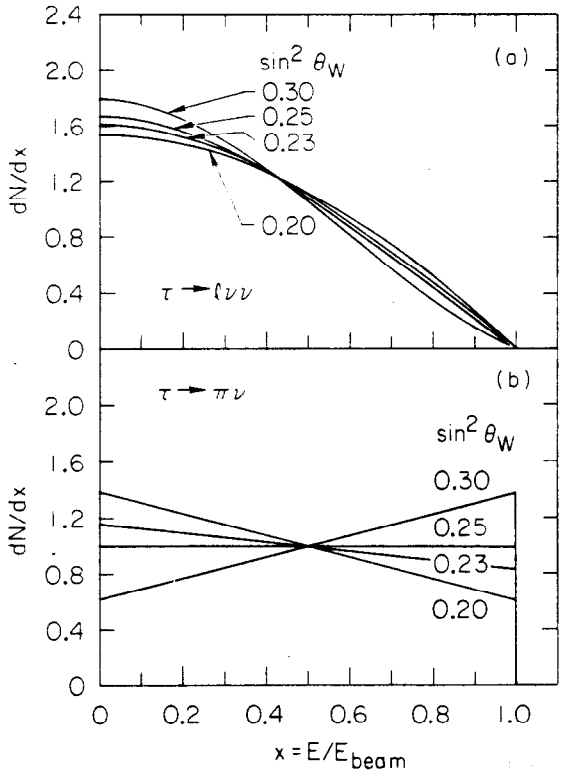

Fig. 14. Momentum spectra for τ decay products for different values of $\sin^2\theta_W$ (a) for charged leptons arising from $\tau \to \ell\nu\bar{\nu}$ and (b) for pions arising from $\tau \to \pi\nu$.

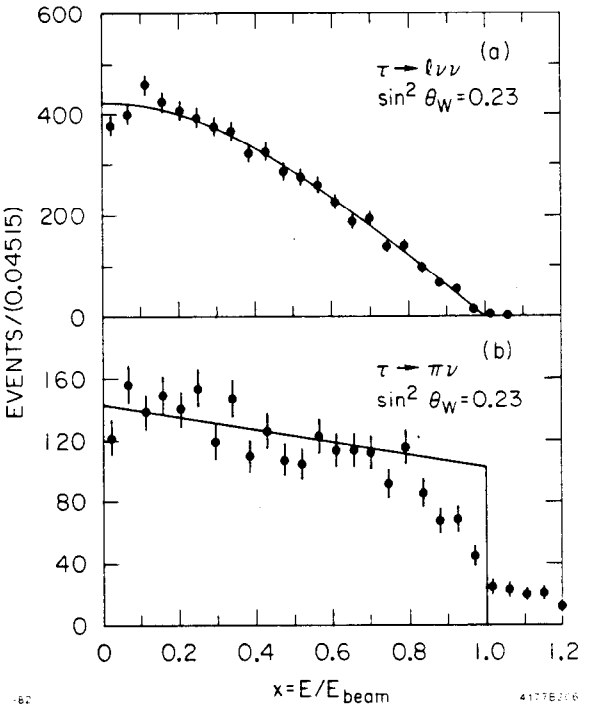

Fig. 15. The solid lines are taken from figure 14 with $\sin^2\theta_W = 0.23$. The data points result from a computer simulation which includes realistic detector components.

For the decay channel $\tau \to \pi\nu$, $P_\tau = 6\langle x \rangle - 3$ and therefore from this simulation

$$P_\tau \approx 0.11$$

$$\delta P_\tau = 6\delta\langle x \rangle = 0.036 \ .$$

Also from the previous discussion we have

$$A^\tau_{F-B} \approx 0.043 \pm 0.008 \ .$$

We obtain the relative sign of a_e and v_e from the ratio

$$\frac{A^\tau_{F-B}}{P_\tau} = -\frac{3a_e v_e}{(a_e^2 + v_e^2)} \ .$$

Clearly our ability to tell the relative sign is limited by the P_τ measurement and hence for this toy experiment one would determine the relative sign of v_e and a_e to $\gtrsim 3\sigma$ from the decay $\tau \to \pi\nu$. Additional statistical power would come from the decay modes $\tau \to e\nu\bar{\nu}$ and $\tau \to \mu\nu\bar{\nu}$.

From $R^{e^+e^-}$ and $A^{e^+e^-}_{F-B}$ one obtains a_e and v_e, their relative sign, coming from the additional measurement of P_τ. Measuring $R^{\mu^+\mu^-}$, $R^{\tau^+\tau^-}$, $A^{\mu^+\mu^-}_{F-B}$ and $A^{\tau^+\tau^-}_{F-B}$ will then provide the μ^- and τ^- vector and axial vector couplings. Having measured all the couplings provides further checks on the Standard Model and in particular of the universality of the Weak Interactions.

Now life becomes much easier if one has a longitudinally polarized electron (or positron) beam. As we discussed in section 2, the SLC is expected to have a longitudinally polarized e^- beam with polarization $P_{e^-} \gtrsim 50\%$. In addition, on a pulse by pulse basis, the sign of the polarization can be switched from left to right. Now one can do a very simple experiment namely to measure the total cross section for left polarized electrons (σ_L) and that for right polarized electrons (σ_R). These cross sections will not be equal and we can form an asymmetry

$$A_{L-R} = \frac{\sigma_L - \sigma_R}{\sigma_L + \sigma_R} = -2P_{e^-}\frac{a_e v_e}{(a_e^2 + v_e^2)} \ .$$

Recognize that A_{L-R} immediately gives the relative sign of v_e and a_e thus obviating the need for the τ polarization measurement. In addition this is a very simple experiment to perform and, unlike the measurement of A_{F-B}, all the Z^0 decay (except $Z^0 \to \nu\bar{\nu}$ of course) events can be used and statistics are no problem at all. For $P_{e^-} = 0.5$ and $\sin^2\theta_W = 0.22$, $A_{L-R} = 12\%$ – three times larger than A^μ_{F-B}. So it will be much easier to measure A_{L-R} on the Z^0 peak than A^f_{F-B}.

The error in A_{L-R} is dominated by the measurement error in P_{e^-}. How do we measure P_{e^-}? Two polarimeters will be built[17] for the SLC one of which is designed to achieve a 1% measurement of P_{e^-}. If 1% were actually achieved, one would find from

$$\frac{\delta A_{L-R}}{A_{L-R}} = \frac{\delta P_{e^-}}{\delta P_{e^-}} \simeq \frac{7.3\delta(\sin^2\theta_W)}{\sin^2\theta_W}$$

that $\delta(\sin^2\theta_W) = 0.0003$. If we consider a more conservative starting error of $\delta P_{e^-}/P_{e^-} \sim 5\%$, we find $\delta(\sin^2\theta_W) \approx 0.0015$. Notice that to get similar precision for A_{F-B} would take 10 times more running! One begins to see why polarized e^- beam at the SLC is a powerful tool. Further examples will follow in the later sections.

6.3 Searching for the Top Quark

How about searching for the particles which should be present in the minimal Standard Model but have not been observed – namely the top quark and the neutral Higgs boson. We discussed already that we might have an indication from the width measurement that top was being produced at the Z^0. To make sure that we have a new, heavy quark being produced at the Z^0 is quite simple, requiring rather little data, as long as the quark mass is $\lesssim 40$ GeV/c^2. Establishing the quark charge (2/3 or $-1/3$) is more of a challenge but, with enough data, this too seems possible.

As we saw in figure 6, the production of $t\bar{t}$ falls with increasing mass. However the experimental problems of isolating $t\bar{t}$ events become easier with increasing mass. Hence, as we shall see, one has roughly equal sensitivity to finding top in the mass range from $M_t = 25$ GeV/c^2 to 40 GeV/c^2. There are too straightforward ways to isolate $t\bar{t}$ events from hadronic events produced via the 5 light quark species. One way is to look at the shape of the events and the other is to measure the transverse momentum (P_t) (measured relative to the quark axis) of leptons produced in the semi-leptonic decay of the t quark. Both methods work because the top quark is so much heavier than the 5 known quarks, which in turn have masses $\ll M_{Z^0}$.

In the former approach suppose we run at the Z^0, collect hadronic events (72% of Z^0 decays) and do a sphericity shape analysis[18] on the events. Hadronic events are very simple to isolate because of their high multiplicity and large detected energy. They will be isolated with high efficiency and no background. The sphericity analysis will provide three orthogonal axes, two of which define a plane – the event plane – which is the plane which contains most of the momentum of the detected particles. The aplanarity is a measure of the momentum out of the event plane. Because transverse momentum (P_t) is limited in the fragmentation

process and because the 5 known quarks will all have high velocities in Z^0 decay, the events containing the 5 known quarks will have small aplanarity. However if a heavy quark is produced it will have a low velocity, and the same limited P_t will result in a considerably larger aplanarity.

The second approach uses the fact that the t quark will have copious ($\sim 10\%$) semileptonic decays. Again because of their heavy mass and low velocity, the leptons arising from such decays make a large angle with respect to the quark (jet) direction. This can be contrasted with leptons arising from the 5 known quarks. Rather than measuring the decay angle, we choose to use the transverse momentum relative to the quark direction (P_t). In an experiment the sphericity (or thrust) axis is a good measure of the $q\bar{q}$ direction and momenta are usually measured relative to this axis. The muons (or electrons) coming from the $t\bar{t}$ events will have substantially larger P_t than the corresponding leptons from the lighter quarks. This second approach is preferred since it is much less sensitive to the Monte Carlo assumptions concerning higher order QCD effect (gluon radiation).

The MARK II Group[19] has studied these two methods for isolating top at the SLC. The simulations were done using the LUND Monte Carlo program. Figure 16 shows the aplanarity distribution for the 5 light quarks arising from 10^4 Z^0 decays and the additional contribution which would result from the production of $t\bar{t}$ with $M_t = 40$ GeV/c^2. One sees a clear $t\bar{t}$ signal for aplanarities > 0.12. Similarly figure 17 contrasts the lepton P_t relative to the thrust axis for leptons arising from the light quarks and the $t\bar{t}$ events ($M_t = 40$ GeV/c^2). For this plot an aplanarity cut of > 0.02 has been applied. A clear $t\bar{t}$ signal is seen. The results of this study are shown in table IV from which we can see that by combining both aplanarity and lepton P_t information, 10^3 Z^0's should be enough to indicate that a new heavy quark ($M \lesssim 40$ GeV/c^2) was being produced at the SLC. With 10^4 events there would be little doubt. 10^3 Z^0's is 4 days of running at $\mathcal{L} = 10^{29}$ cm^{-2} sec^{-1}.

For studying $t\bar{t}$ events, we note that the high P_t tag will provide $\sim 10^4$ $t\bar{t}/10^6$ Z^0's, with the additional attractive feature that the sign of the lepton's electric charge distinguishes the q vs $\bar{q}$ source for the lepton. This is crucial for studying the charge asymmetry A^t_{F-B}.

How about measuring the t quark mass? A measurement with an accuracy of a few GeV will result from fitting the shapes of the aplanarity and P_t spectra. This method however suffers from the fact that it relies heavily on the input to the Monte Carlo in particular to how one models the quark fragmentation process and the higher order QCD effects. Measuring the jet mass doesn't work well because with the "fat" tt events, assignment of particles to the t and $\bar{t}$ is ambiguous and the $t\bar{t}$ production direction is not well specified, especially for large t masses. In principle the best method of determining the t quark mass is

to return to figure 6, the t quark threshold curve. If one could find out where one was on the curve, one could "read off" M_t. This method is discussed fully in reference 20, briefly here.

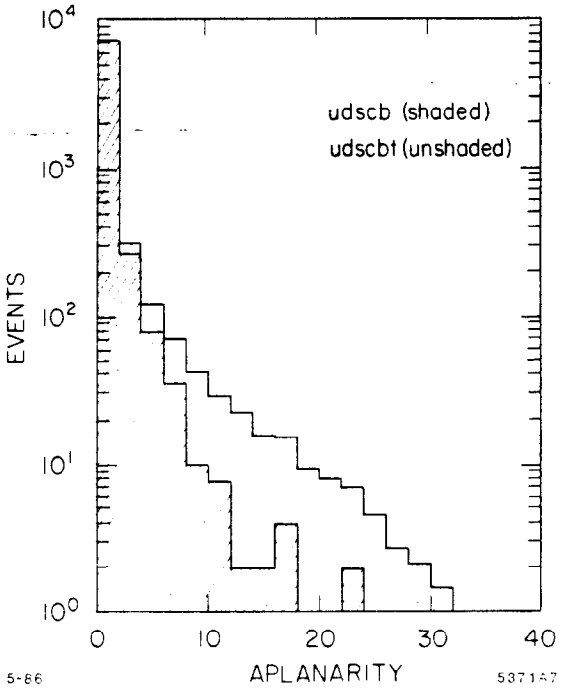

Fig. 16. The aplanarity distribution for hadronic events at the Z^0 contrasting the contribution from the five light quarks (shaded) with that coming from $Z^0 \rightarrow t\bar{t}$ where $M_t = 40$ GeV/c^2.

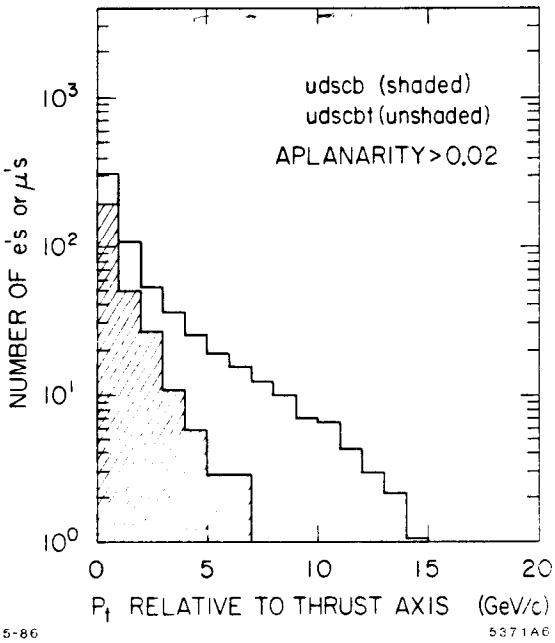

Fig. 17. The P_t spectrum for leptons arising from Z^0 decays to the five light quarks (shaded) contrasted with leptons arising from $Z^0 \rightarrow t\bar{t}$ with $M_t = 40$ GeV/c^2.

TABLE IV

	# Events Produced	Detected # Events with Aplanarity > 0.12	# e, μ with $P_t > 3$ GeV/c and Aplanarity > 0.02
Background; LUND *udscb*	7200	9	17
$t\bar{t}$; $M_t = 30$ GeV/c^2	634	48	146
$t\bar{t}$; $M_t = 35$ GeV/c^2	452	64	131
$t\bar{t}$; $M_t = 40$ GeV/c^2	265	58	88
$t\bar{t}$; $M_t = 45$ GeV/c^2	83	13	27

Recall $\rho = \Gamma_t(\beta)/\Gamma_u$ as plotted in figure 6. Let $r = N_h/N_{\mu\mu}$ where N_h is the number of hadronic events and $N_{\mu\mu}$ is the number of $\mu^+\mu^-$ events. Then

$$\rho = 1 + r\,\frac{\Gamma_{\mu\mu}}{\Gamma_u} - \frac{\Gamma_h}{\Gamma_u}$$

where Γ_h = the hadronic width calculated in the Standard Model for 3 quark generations of massless colored weak isospin doublets. $\Gamma_{\mu\mu}$ and Γ_u are the partial widths for the $Z^0 \to \mu^+\mu^-$ and $Z^0 \to u\bar{u}$. The experiment is simple – measure r which provides ρ which from figure 6 provides M_t. The measurement of r does not involve a luminosity measurement and should be free of systematics at the 1-2% level. If we assume our canonical 10^6 Z^0, $N_h \approx 730{,}000$, $N_{\mu^+\mu^-} \approx 31{,}000$ and if $\sin^2\theta_W$ is known to ≈ 0.001 then one obtains a t mass resolution shown in figure 18.

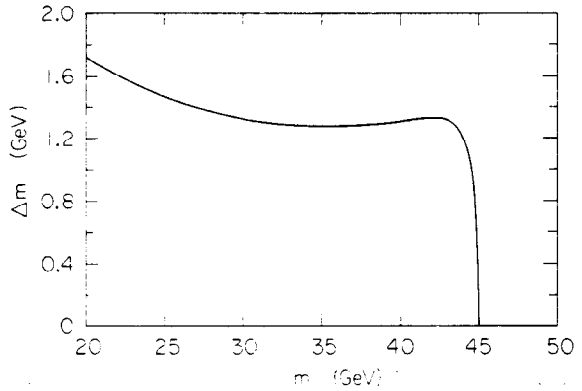

Fig. 18. The error in the determination of the top quark mass as a function of the top quark mass for a sample of 10^6 Z^0 events. No systematic errors are included in this plot.

Notice that in order to use this method one requires independent knowledge that $t\bar{t}$ events are being produced at the Z^0 and that there are no other processes which are contributing to N_h.

Suppose such a heavy quark is found. How does one know that it is indeed the $q = 2/3$ t quark as opposed to a 4th generation $q = -1/3$ b' quark? To distinguish these two possibilities requires measuring A^q_{F-B} which is 6.5% (13%) for $q = 2/3$ $(-1/3)$. We will discuss this later in section 6.6.

6.4 Searching for the Neutral Higgs, H^0

At the Bonn Conference in 1981, Okun said[21] that in his mind the outstanding experimental challenge was the search for scalars. He urged experimentalists to "drop everything" and devise cunning searches for the elusive scalars. To date no search has proven successful and it is interesting to speculate how one could search for the H^0 running on the Z^0.

—The H^0 will couple to the heaviest fermions available and this feature will be used in any search for the H^0. The decay rate for $H^0 \to f\bar{f}$ is given by:

$$\frac{d\Gamma}{d\Omega} = \frac{G_F M_{H^0} m_f^2}{16\pi^2\sqrt{2}}$$

The decay rate depends on m_f^2 (m_f is the fermion mass) and is isotropic. So if $M_{H^0} < 2M_b$, the H^0 will decay mostly to $c\bar{c}$ and $\tau^+\tau^-$. If $2m_t < M_{H^0} < 2M_b$ then the H^0 will decay mostly to $b\bar{b}$. These conclusions are summarized in figure 19.

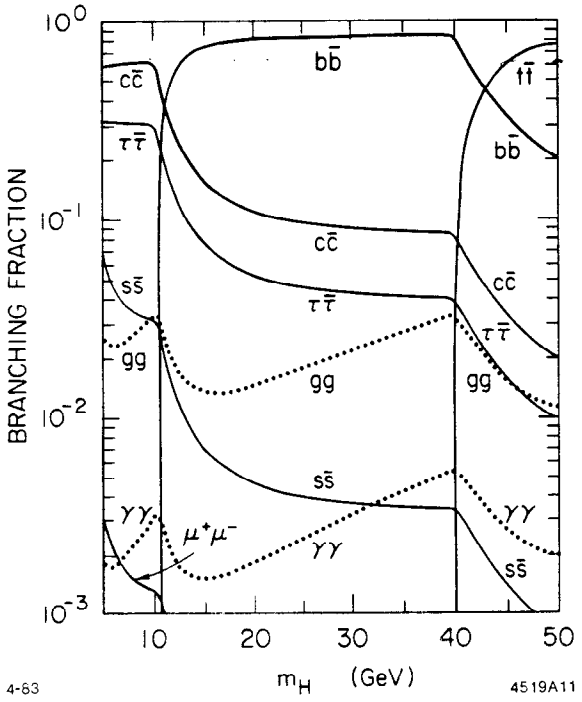

Fig. 19. Decay modes of the neutral Higgs boson as a function of its mass.

How can we search for the H^0? The process $e^+e^- \rightarrow Z^0 \rightarrow H^0H^0$ is forbidden by spin-statistics. The process $Z^0 \rightarrow H^0\gamma$ vanishes in first order because the Z^0 and γ are "orthogonal" – in second order the rate is too small to be of any practical use. The most promising search channel seems to be $Z^0 \rightarrow H^0Z^{0*} \rightarrow H^0\ell^+\ell^-$ (see figure 20) which was first discussed[22] by Bjorken and is also discussed in reference 23. The rate for this process is given by:

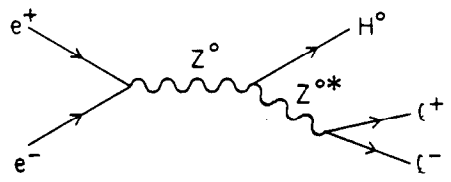

Fig. 20. The process $e^+e^- \rightarrow Z^0 \rightarrow H^0\ell^+\ell^-$.

$$\frac{1}{\Gamma(Z^0 \rightarrow \mu^+\mu^-)} \frac{d\Gamma(Z^0 \rightarrow H^0\ell^+\ell^-)}{dM_{\ell^+\ell^-}} = \frac{\alpha F}{4\pi \sin^2\theta_W \cos^2\theta_W}$$

where

$$F = \frac{10k^2 + 10\lambda^2 + 1 + (k^2 - \lambda^2)[(1 - k^2 - \lambda^2) - 4k^2\lambda^2]^{1/2}}{(1 - k^2)^2}$$

$$M_{\ell^+\ell^-} = \text{lepton pair mass}$$

$$k = M_L/M_{Z^0}$$

and $$\lambda = M_{H^0}/M_{Z^0} \quad .$$

This relative rate, integrated over $M_{\ell^+\ell^-}$, is plotted as a function of M_{H^0} in figure 21. Also shown for comparison is the rate for $Z^0 \rightarrow H^0\gamma$. $B(Z^0 \rightarrow \mu^+\mu^-) = 3\%$, so one sees that for $M_{H^0} \approx 20$ GeV/c^2 $B(Z^0 \rightarrow H^0\ell^+\ell^-) \approx 3 \times 10^{-5}$, a yield of 30 events for 10^6 Z^0 events. Unfortunately the rate drops off very rapidly with increasing H^0 mass and for masses above $\sim$ 40 GeV/c^2 the measurement becomes severely rate limited.

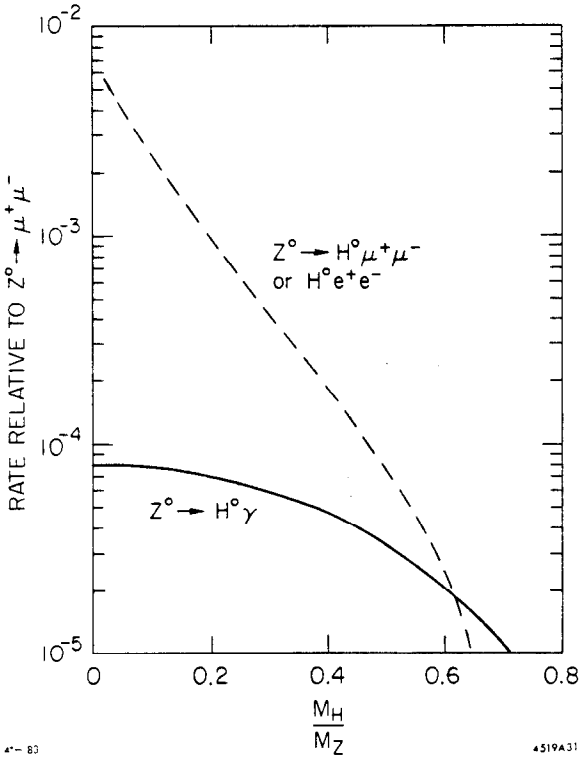

Fig. 21. The decay rate for $Z^0 \rightarrow H^0e^+e^-$ or $Z^0 \rightarrow H^0\mu^+\mu^-$ relative to $Z^0 \rightarrow \mu^+\mu^-$ which has a branching fraction of 3%.

The $H^0\ell^+\ell^-$ signal must be sought in the presence of an enormous background from $Z^0 \rightarrow$ hadrons. For $M_{H^0} \approx 20$ GeV/c^2 there are $\approx 10^4$ $Z^0 \rightarrow$ hadron events per $Z^0 \rightarrow H^0\ell^+\ell^-$ event! Luckily the event topology is very favorable and a measurement indeed seems possible. Many of the detector groups at SLC and LEP have studied the experimental problems and their conclusions are pretty uniform. We chose here the study discussed in the MARK II proposal.[12]

The favorable topology arises from the fact that most of the energy in the process $Z^0 \rightarrow H^0\ell^+\ell^-$ goes to the virtual Z^0 and hence the two leptons which result from the decay of the virtual Z^0 have very high invariant mass and momenta. The H^0 is produced with a fairly small fraction of the available energy and will decay mostly into two quark jets. In addition there is very little correlation between the H^0 direction and the e^+ or e^- direction and in most events the $e^\pm$ will be well separated from the H^0 decay products. The topology is schematically shown in figure 22.

The main source of background comes from the process $Z^0 \rightarrow t\bar{t}$ where both the t and $\bar{t}$ decay semi-leptonically. However requiring the angle between sphericity axis of the hadronic system (all particles except the ℓ^+ and ℓ^-) and the leptons to be $\gtrsim$ 200 mrad virtually eliminates this background for $M_{H^0} \lesssim$ 40 GeV/c^2. This cut loses very little signal ($\approx$ 6%) because there is virtually no correlation between the direction of the leptons and the hadronic sphericity axis.

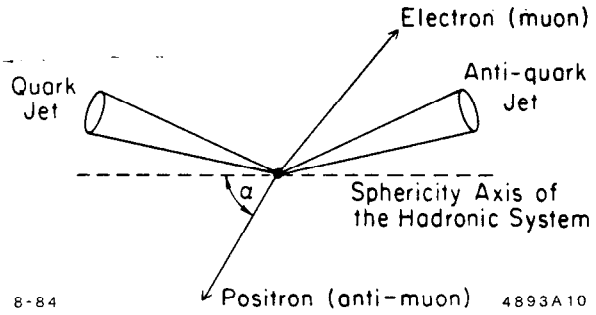

Fig. 22. A schematic representation of the topology of the $Z^0 \rightarrow H^0\ell^+\ell^-$ events.

The mass of the hadronic system (the H^0) is obtained from the missing mass recoiling against the lepton pair. The experiment can be done with either a e^+e^- or $\mu^+\mu^-$ lepton pair providing that the energy resolution of the leptons is sufficiently good to see a peak in the missing mass. The missing mass recoiling against the e^+e^- ($\mu^+\mu^-$) pair is shown in figure 23 (24) for the MARK II simulation for Higgs masses of 10, 25 and 35 GeV/c^2. Clear signals are seen. The main issue for this measurement will be statistics. For Higgs masses of 10, 20, 30 and 40 GeV/c^2 one expects to have 180, 50, 25 and 10 events produced in the $H^0e^+e^- + H^0\mu^+\mu^-$ channels per 10^6 Z^0 events.

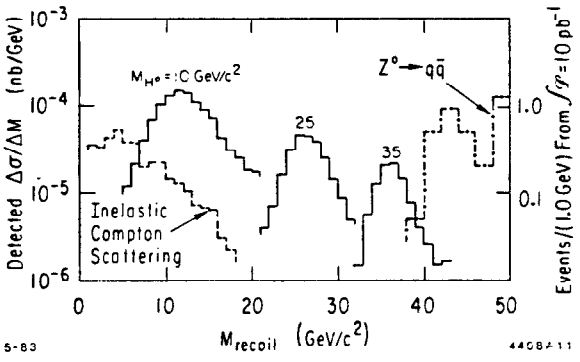

Fig. 23. The Higgs signal from $Z^0 \rightarrow H^0e^+e^-$. The expected backgrounds are also shown.

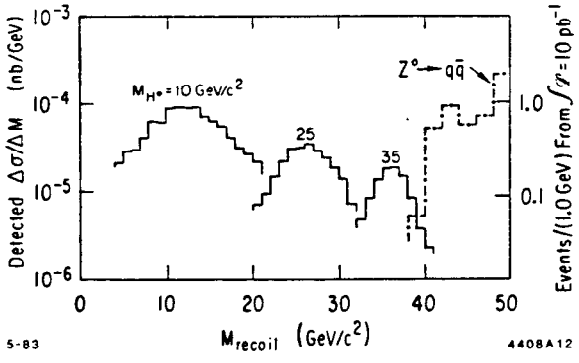

Fig. 24. The Higgs signal from $Z^0 \rightarrow H^0\mu^+\mu^-$. The expected backgrounds are also shown.

Assuming the search was successful and we found a peak in the recoil mass spectrum how do we know that we have discovered the Higgs scalar? We would have to verify that it decayed isotropically and that the couplings favored the heaviest fermion pair available.

We can measure the decay angular distribution as follows. First we would reconstruct the two jet directions from the particles associated with the jets. From the ℓ^+ and ℓ^- momenta we can reconstruct $\vec{P}_{H^0}$. Knowing M_{H^0} and $\vec{P}_{H^0}$, we can transform the jet directions into the H^0 center of mass and plot the decay angular distribution. (This method will work as long as we can make the assumption that the decay angular distribution is symmetric about $\theta^* = 90°$. This is because we don't know how to distinguish the jet from the anti jet (θ^* from $\pi - \theta^*$) and hence by plotting both we are assuming a symmetric decay distribution). Realistically the major problem with this procedure will be the limited statistics. Optimistically one might have ≈ 50 events to play with.

Now how about measuring if the coupling is proportional to m_f^2? Here the procedure would depend on M_{H^0}. Suppose, as is likely, that $M_{H^0} > 10$ GeV/c^2 in which case $H^0 \to b\bar{b}$ almost exclusively (see figure 19). We will see in the next section that using a vertex detector one can expect to tag events containing two b jets with an efficiency $\gtrsim 50\%$ and this with very little contamination from c jets. This can be done because the b quark has a long measured ($\sim$ psec) lifetime. So one would subject the $H^0\ell^+\ell^-$ candidate events to this test and if indeed half (= tag efficiency) the events were tagged as having a b jet, one would feel fairly confident that the H^0 decayed predominantly to $b\bar{b}$. If $M_{H^0} < 10$ GeV/c^2 the obvious signal to look for would be $H^0 \to \tau^+\tau^-$.

To summarize the H^0 search then, it is probable that if $M_{H^0} \lesssim 40$ GeV/c^2 it can be found at the Z^0 . We will require a machine with excellent luminosity – $\langle\mathcal{L}\rangle > 10^{30}$ cm^{-2} sec^{-1} – and a detector with good electromagnetic calorimetry and/or momentum resolution. All the LEP and SLC detectors appear capable of doing this measurement. With sufficient statistics ($\gtrsim 50$ events) the H^0 decay angular distribution and coupling can probably be inferred.

6.5 What Will We Learn From $Z^0 \to$ Hadrons?

An obvious question is can we learn anything form $Z^0 \to$ hadrons which cannot be obtained from PETRA ($E_{c.m.} \lesssim 46$ GeV) and PEP ($E_{c.m.} \lesssim 36$ GeV)? The answer is yes and probably the main reason is that the Z^0 offers a very large statistical advantage over the PEP and PETRA machines. At present the largest PEP/PETRA hadronic dataset is the MARK II which has 100,000 hadronic events at a PEP energy of $E_{c.m.} = 29$ GeV. It has taken three years to accumulate this data and the present performance of PEP is that a good PEP year is worth 60,000 hadronic events. Contrast this with the expectation that a good SLC/LEP year will yield $\approx 180 \times 10^4$ hadronic events or 30 times as much as PEP. So there will be a considerable improvement in statistics. We now examine some of the physics which will be covered. (We should note that at

present the PEP machine is being upgraded. It will return to service in Fall 87 with an expected improvement in $\langle \mathcal{L} \rangle$ of a factor of 5.)

QCD Tests

As discussed by the authors in reference 24 (and probably many others) the QCD corrections to the Z^0 hadronic final states are exactly these calculated for lower energy e^+e^- interactions. In particular one recovers the familiar Sterman-Weinberg formula. All the usual low energy tools like sphericity, thrust, etc. are equally useful at the Z^0. The familiar 3 jet Dalitz plot distributions for $e^+e^- \rightarrow Z^0 \rightarrow qqg$ are the same as for the continuum:

$$\frac{d^2\Gamma(Z^0 \rightarrow 3 \text{ jets})}{dx_1 dx_2} = \Gamma(Z^0 \rightarrow \text{hadrons}) \frac{2\alpha_s(M_Z)}{3\pi} \frac{(x_1^2 + x_2^2)}{(1-x_1)(1-x_2)}$$

where x_i $(i = 1,2,3)$ are the fractional parton energies $(x_i = 2E_i/E_{c.m.})$ and $\sum_i x_i = 2$. We can study the three jet events at the Z^0 in much the same way as we study them at PETRA and PEP. These studies will probably be easier at the Z^0 because the jet cone angles will be $\sim$ 2-3 times smaller $(\approx 1/E_{\text{jet}})$ than at PEP or PETRA. Hence the problems of which particles belong to which jet should be easier. This will provide more reliable measurements of x_i, quark and gluon jet multiplicities and jet directions. In addition the efficiency for finding well reconstructed 3 jet events should be higher than at lower energies. And of course there will be a copious supply of 3 jet events. Simulations have shown that about 60% of the produced three jet events are cleanly reconstructed which would yield about 5×10^4 reconstructed 3 jet events/10^6 produced Z^0's. By contrast the MARK II has about 5×10^3 reconstructed 3 jet events and many of the PETRA results at 34 GeV have been published on $\lesssim$ 1000 3 jet events. Back to what we will learn.

We will try to measure α_s, a task which has been difficult at lower e^+e^- energies.[25] Part of the problem with the lower energy measurements has been understanding the QCD corrections and removing the model dependence. Combining the new data at $E_{c.m.} = M_{Z^0}$ with the low energy data will allow one to measure some of these effects which are now parametrized in a variety of models. α_s would be measured using the same techniques as at lower energies (see reference 25 as an example) namely studying the Dalitz plot distributions, or measuring the ratio of 3 jet to 2 jet events, or measuring particle energy correlations, event shapes, etc. I expect the model dependent problems encountered at lower energies will be much improved at the Z^0 . However new model dependent effects may prove troublesome, an example of which is the appearance, at higher energies, of many soft gluons. I would not speculate with confidence that α_s will be more easily measured at the Z^0 , but in all probability things will be better. With many reconstructed jets at energies hitherto not available in e^+e^- , more

information will be gained on the parton fragmentation process. In particular the question of whether quarks and gluons fragment differently can be studied. It has been argued in many places (see reference 26 for but a few) that for highly perturbative parton regimes (high energy partons) gluon jets should be considerably broader than quark jets. This is an important test because it arises from the gluon self-coupling which relates directly to the non-abelian nature of QCD. The difference in the fragmentation of quarks and gluons comes about from the fact (see figure 25) that the color charge at the triple gluon vertex is 9/4ths larger than at the quark-quark-gluon vertex. The ratio of the cone angle δ (a la Sterman and Weinberg) of a gluon and a quark jet is given roughly by

$$\delta_g(E) \approx \delta_q(E)^{4/9}$$

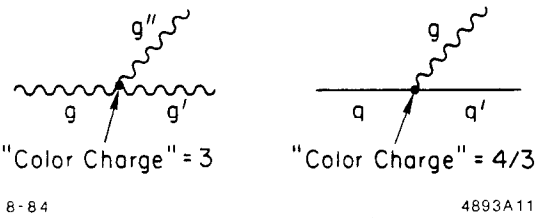

Fig. 25. The contrasting "strengths" of the triple gluon vertex and the quark-quark-gluon vertex.

where δ is measured in radians. The cone angle δ is such that most ($\gtrsim 90\%$) of the parton energy is contained in the cone. At the Z^0 one expects $\delta_q \simeq 10°$ which would imply a gluon jet of the same energy would have $\delta_g \approx 27°$. Such large differences should be seen easily and the Z^0 3 jet events should provide a meaningful test of differences in quark and gluon jets.

Flavor Tagging

We have already seen earlier in this section that $t\bar{t}$ events can easily be tagged using event shape parameters or high P_t leptons. The advantage of the high P_t tag is that the sign of the lepton charge flags which jet is t and which is the $\bar{t}$. The importance of this will become apparent soon. Studies by the MARK II Upgrade Group[19] have shown that the high P_t lepton tag has high efficiency for selecting $t\bar{t}$ events and in addition backgrounds (from $b\bar{b}$ mainly) are small. Requiring a high P_t lepton they find $\approx 10^4$ tagged $t\bar{t}/10^6$ Z^0's with a background of $< 10\%$.

How about tagging $b\bar{b}$ events? The B meson appears[27] to have a lifetime on the order of 1 psec. At the Z^0, they will travel $\gamma\beta c\tau \approx 3$ mm on average before they decay. The decay particles of the B meson, when extrapolated back towards the primary vertex, will appear to "miss" the primary vertex (see figure 26). The amount by which they "miss" is called the impact parameter, b. Large impact parameter tracks will signal the decay of a long lived particle. From simulations one finds that for $\tau_B = 10^{-12}$ secs typical tracks from B meson decay in $Z^0 \rightarrow b\bar{b}$ events have $b \gtrsim 200\ \mu$. This can be contrasted with expected measurement errors of 50-100 μ. In a study done by the MARK II Upgrade Group,[28] efficiencies of

$\geq$ 50% were found for tagging events of the type $Z^0 \rightarrow b\bar{b}$. The technique used was to require at least 3 tracks in a jet with $\geq 3\sigma_b$ where σ_b was the error in the measurement of the track's impact parameter. Multiple scattering in the apparatus walls can cause tracks to have large impact parameters and hence provide bogus tagging information. Requiring three tracks with a substantial impact parameter alleviates this problem. In addition the invariant mass of the three large impact parameter tracks was required to be > 1.95 GeV/c^2 which eliminates almost all background from D decays. The tagged $b\bar{b}$ events sample was found to have $< 10\%$ background from non $b\bar{b}$ events.

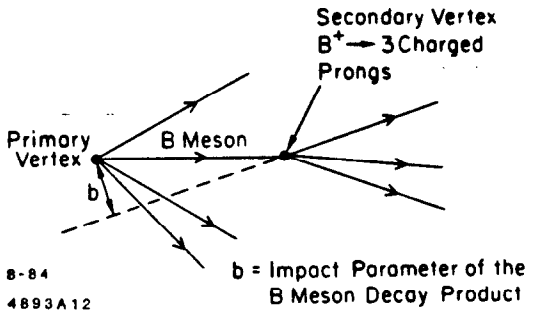

Fig. 26. The production and subsequent decay of a B meson indicating the primary vertex, secondary vertex and the impact parameter b of one of the B decay tracks.

Using this efficiency as prototypical, one would expect 6.8×10^4 tagged $b\bar{b}$ events/10^6 Z^0 events. If in addition one required an electron or a muon to distinguish quark and antiquark b jets, one would have a tagging efficiency of about 8×10^3 $b\bar{b}/10^6$ Z^0 events.

So it seems as if one will be able to tag b and t jets at the SLC and LEP with impressive event yields. What physics can be done? Clearly the fragmentation process, both longitudinal and transverse, for heavy quarks can be studied. Jet multiplicity can be studied. Comparisons with low energy data will provide additional information on the fragmentation process.

The B lifetime will be measured with better precision and better statistics than at PEP. Current τ_B measurements rely on $\lesssim 1000$ events which affects not only the statistical error in τ_B but also limits the ability of the experiments to understand their systematics. Presently the systematics are limiting the measurements at the $\sim 25\%$ level. We can use the tagged $b\bar{b}$ events to measure the B meson lifetime and divide the events into two jets. The one jet will provide the b jet tag as discussed above. The other jet can be used in an unbiased way to measure the B lifetime. Estimates from simulations done by the MARK II Upgrade Group indicate that using the same method employed at PEP[27] a systematic error of $\sim 5\%$ should be achieved for τ_B.

— With tagged $b\bar{b}$ and $t\bar{t}$ events we could measure the charged 2/3rds and $-1/3$rd quark couplings. Recall (section 4) that if we measure

$$R_q = \frac{\sigma_{q\bar{q}}}{\sigma_{\text{point}}} \propto (a_q^2 + v_q^2)$$

and

$$A^q_{F-B} = \frac{3a_e v_e a_q v_q}{(a_q^2 + v_q^2)(a_e^2 + v_e^2)}$$

we can obtain a_q and v_q. (We are assuming a_e, v_e are measured as discussed earlier in this section.) With a tagged sample of $b\bar{b}$ and $t\bar{t}$ we can make these measurements. For the forward–backward asymmetry we need to distinguish q from $\bar{q}$, so we will have to use events with an electron or muon. Even with this restriction the statistical errors in the measurement of the couplings will be $\lesssim 2\%$ for 10^6 Z^0 events. The R_q measurement requires an accurate measurement of luminosity which will be possible at the $\leq 5\%$ level. In order to determine the quark direction one will use the thrust axis. At the Z^0 this will be well determined (except for $t\bar{t}$ as $M_t \to 40$ GeV/c^2) and should not effect the quality of the measurement of A^q_{F-B}. It will be very important to have good detector coverage at small θ angles. The solid angle (25% of 4π) for which $\theta < 40°$ contains as much asymmetry information as the remaining 75% of 4π. Based on those considerations, I would expect one could measure the b couplings to $\lesssim 10\%$. A^t_{F-B} is a little bit trickier, especially as $M_t \to 40$ GeV/c^2. In this case it becomes harder to define the thrust axis and the correlation between the sign of the lepton charge and the parent (t or $\bar{t}$) becomes weaker. Nonetheless in the MARK II simulation[19] of A^t_{F-B} for $M_t = 40$ GeV/c^2, a 4σ effect was seen for an equivalent sample of 3×10^5 produced Z^0's. These measurements of A^b_{F-B} and A^t_{F-B} will constitute important tests of the Standard Model in the quark sector.

We return now to the question posed earlier. Suppose we discover a new heavy quark at the SLC or LEP. How do we know its charge? Is it the t or a b'? The key is the difference in the couplings. Simple substitution using the values in table I gives

$$A^t_{F-B} = 6.5\%$$

and

$$A^b_{F-B} = 13\% \quad .$$

The simulation discussed above provides a $\sim 4\sigma$ differentiation for 3×10^5 produced Z^0's.

The tagged $b\bar{b}$ sample will be an excellent place to search for mixing in the neutral B meson system. The method would be to search for hadronic events which contain leptons of the same sign in opposite hemispheres. This would result from the production of $B^0\bar{B}^0$ where, through mixing, the B^0 ($\bar{B}^0$) evolves to a $\bar{B}^0$ (B^0). Both B mesons are then required to decay semi-leptonically.

Very little mixing is expected[29] to occur in the B_u mesons. However maximal (100%) mixing could be possible in the B_s mesons. We can make a crude estimate

of the number of same sign dileptons we would have for 10^6 Z^0's. Assuming that the mixing is maximal in the B_s system, that the fraction of B_s produced is 15% and that $B(b \to \ell x) = 10\%$ one would have:

$$\begin{aligned} \#\text{ same sign } e^{\pm}e^{\pm} &= (.1)^2 \times (.15) \times 7 \times 10^4 \\ &\simeq 100 \quad . \end{aligned}$$

Here 10^6 Z^0's will provide $\sim$ 400 same sign dilepton (ee, $\mu\mu$ and $e\mu$) events. The backgrounds for these events should be small because the hadron rejection capabilities of the SLC and LEP detectors will be excellent. Charm backgrounds are all but eliminated by the $b\bar{b}$ tag as explained above. The SLC and LEP could well be the best hunting ground in the near future for $B^0 - \bar{B}^0$ mixing effects.

7. Z^0 PHYSICS BEYOND THE STANDARD MODEL

Possibly to most interesting physics at the Z^0 will be the surprises. Certainly we all hope so! How about some "predictably" surprises – namely things which spoil the tidy Standard Model predictions?

7.1 NON-MINIMAL HIGGS SCHEME; SEARCHING FOR CHARGED AND NEUTRAL HIGGS

We have, until now, considered the minimal Higgs structure of one Higgs doublet. However there is nothing in the Standard Model which prevents us from having more than one Higgs doublet. With two Higgs doublets (8 fields) one gives up three of these fields to produce masses for the $W^{\pm}$ and Z^0, leaving 5 physical Higgs particles. They are:

Two neutral scalars	H_1^0, H_2^0
One pseudoscalar	h^0 (the axion in some models)
and two charged pseudoscalars	H^+, H^- .

For decay purposes the usual scalar rule applies – couplings are largest for the heaviest fermion decay products permissable.

— The search for the two neutral scalars proceeds exactly as discussed earlier for H^0 except that now the lower 7.5 GeV/c^2 bound on the H^0 mass is removed. Looking for H^0's below 7.5 GeV/c^2 has the advantage of increasing production rate (see figure 21). However at masses of a few GeV/c^2, two photon backgrounds become a major nuisance.

What about searching for the $H^{\pm}$. The only process available at the Z^0 is $e^+e^- \rightarrow Z^0 \rightarrow H^+H^-$ which has a rate of $\Gamma(Z^0 \rightarrow H^+H^-) = \frac{1}{4}\beta^3_{H^{\pm}}(3\%) \simeq 10^{-2}\beta^3_{H^{\pm}}$, where $\beta_{H^{\pm}}$ is the charged Higgs' velocity. From PETRA measurements we know that $M_{H^{\pm}} > 15$ GeV/c which means that the dominant decay mode for the $H^{\pm}$ will be $H^{\pm} \rightarrow b\bar{c}$. (There will also be a small fraction of $H^{\pm} \rightarrow \tau^{\pm}\nu_{\tau}$.) So most of the events arising from $Z^0 \rightarrow H^+H^-$ would contain four jets, two in each hemisphere. The major background comes from QCD 4 jet events of the type $qqgg$ which occur at a rate $\sim \alpha^2 \times 0.72 \simeq 1.5 \times 10^{-2}$. The major handle one has in rejection of this background is that the signal has 4 long-lived quarks whereas at least half the background has only two long-lived quarks. Hopefully a good vertex detector will provide the necessary background rejection.

The $H^{\pm}$ mass would have to be obtained from the di-jet masses in the two hemispheres. Presumably one would have sensitivity up to charged Higgs masses of $\lesssim 40$ GeV/c^2.

7.2 The Generation Puzzle – Searching for New Generations

The discovery of the τ and the b quark has led to a very beautiful symmetry between the quark and lepton sectors. Nature at present appears to have three generations of both quarks and leptons. While this symmetry is indeed attractive, we are led to an obvious question – why three generations? Why not five or ten? We readily understand the need for one generation – our very being is dependent on it. But more than one generation seems superfluous and it is interesting to speculate on why nature chose to replicate itself in this strange way.

The distinguishing generation element is mass – successive generations have higher masses. A perfectly defensible reason why we see three generations then is that the energy of our machines is not sufficient to yield the next generation(s). The prospect of higher energy machines implies more quarks and leptons. We may go to our theoretical friends and ask them where we need to look; where will the next generation appear? The answer is that none of the current theories understands the generation puzzle and no mass predictions exist.

The prospect of a factor of $\gtrsim 2$ in available energy, plus the large rate makes the Z^0 a good place to look for new generations. How do we search for new generations? There are three obvious possibilities:

a) Search for a new charged lepton, $L^{\pm}$,

b) Search for a new $Q = -1/3$ quark, and

c) Search for more ν's.

We do not include searches for $Q = 2/3$ quarks because if such a quark were found, it would satisfy our need for the top quark. Consider the search for $L^{\pm}$.

The $W^{\pm}$ which mediate the decays of $L^{\pm}$ is democratic with respect to fermion coupling strengths. Allowing for three quark colors we have

$$B(L^{\pm} \to \ell^{\pm}\nu\nu) = \frac{1}{12} = 8\%$$

and

$$B(L^{\pm} \to \text{hadrons}) = 76\% \quad .$$

(These numbers will be modified slightly by QCD corrections but, for the argument being made here, these small modifications are unimportant.) We will therefore be able to use the standard low multiplicity searches for $L^{\pm}$ which will be produced in pairs with $B(Z^0 \to L^+L^-) = 3\%\ \beta_{L\pm}(3-\beta_{L\pm}^2)/2$ where β_L is the heavy lepton velocity. It would be like searching for the τ all over again. From PETRA we know that $M_{L\pm} > 18$ GeV/c^2 and hence $\beta_{L\pm} \leq 0.92$. As an example one might search for acoplanar $e^{\mp}\mu^{\pm}$ events. For $M_{L\pm} = 40$ GeV/c^2 ($\beta_L = .4$), there would be 200 $e^{\pm}\mu^{\mp}$ events/10^6 Z^0 events. In the channel acoplanar ex or μx there would be 2.5×10^3 events/10^6 Z^0 events. τ pair production is not a serious background because, while the charged particle multiplicity topology is the same, the decay products of the (light) τ are entirely back-to-back (*i.e.* coplanar) unlike those coming from the $L^{\pm}$. So it is easy to search for $L^{\pm}$ at the Z^0 as long as $M_{L\pm} < M_{Z^0}/2$.

We have already discussed how to find a new heavy quark and how the charge asymmetry A_{F-B} can be used to separate charge $-1/3$ and charge $2/3$ quarks. If a new heavy quark were found with a charge $-1/3$ this would signal the presence of a new generation.

Finally we discuss the search for additional ν's. We derived in section 4 $\Gamma(Z^0 \to \nu\bar{\nu}) \simeq 170$ MeV and decided in section 6.1 that we could possibly measure Γ_{Z^0} with a precision ≈ 50 MeV. But how do we know that the additional width comes from a 4th ν? Is there a way to count the number of ν species?

The answer is yes, but not by running on the Z^0, but rather by running above the Z^0 and observing the radiative transition

$$e^+e^- \to \gamma Z^0$$
$$\qquad\qquad \hookrightarrow \nu\bar{\nu} \quad .$$

One can chose an $E_{c.m.}$ such that the mass recoiling against the photon is M_{Z^0}. In this way one gets an enhanced event rate. This measurement is discussed by Barbiellini et al.[30] and the theoretical background can be found in reference 31. The Feynman diagrams are shown in figure 27. It turns out that the $W^{\pm}$ exchange

diagrams are very small (see figure 28) and can be ignored. If this is done then

$$\frac{d^2\sigma}{dxdy} \simeq \frac{G_F \alpha S f(x,y)(v_\nu^2 + a_\nu^2) N_\nu}{\{[1 - S(1-x)/M_Z^2]^2 + \Gamma_Z^2/M_Z^2\}}$$

where

$$f(x,y) = \frac{(1-x)[(1-x/2)^2 + x^2y^2/4]}{6\pi^2 x(1-y^2)}$$

and

$$x = 2E_\gamma/E_{c.m.} \quad , \quad y = \cos\theta_\gamma$$

$$N_\nu = \#\text{ of } \nu \text{ species} \quad .$$

A measurement of $\sigma_{\nu\bar{\nu}} = \int \frac{d^2\sigma}{dxdy}\, dxdy$ measures directly the number of neutrino species in the world! Each new species adds about 33% to $\sigma_{\nu\bar{\nu}}$. We need to chose $E_{c.m.}$ sufficiently high so that the backgrounds from $e^+e^- \to e^+e^-\gamma$ are sufficiently small. Choosing[30] $E_{c.m.} = 105$ GeV and integrating over $y = \cos\theta_\gamma$ in the interval $20° < \theta_\gamma < 160°$ yields the differential cross section shown in figure 28. We can now integrate over the Z^0 reflection peak, namely require experimentally that one sees a photon of energy 14 ± 2.5 GeV. The cross section so obtained is $\sigma_{\nu\bar{\nu}} = 0.025$ nb for $N_\nu = 3$. Each new generation will contribute $\sigma_{\nu\bar{\nu}} \simeq 0.008$ nb. For $\langle\mathcal{L}\rangle = 3 \times 10^{30}$ cm^{-2} sec^{-1} the event rate is $2/\text{day}/\nu$ species. A 50 day run would yield 100 events/ν species – easily enough to measure N_ν.

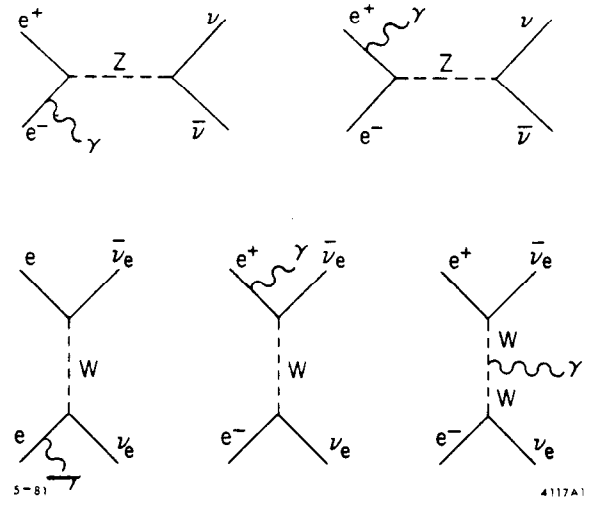

Fig. 27. Lowest order Feynman diagrams contributing to the process $e^+e^- \to \gamma\nu\bar{\nu}$.

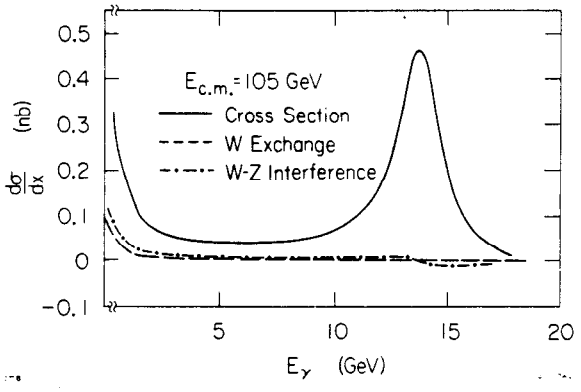

Fig. 28. The differential cross section $d\sigma/dx$ ($x = 2E_\gamma/E_{c.m.}$) is shown as a function of E_γ for the process $e^+e^- \to \gamma\nu\bar{\nu}$. The calculation assumes $E_{c.m.} = 105$ GeV.

The experimental signal is very simple – one hard ($E_\gamma = (14 \pm 2.5)$ GeV) photon in the angular range $20° < \theta < 160°$ and nothing else. What about backgrounds from QED processes like $e^+e^- \rightarrow e^+e^- \gamma$ and $e^+e^- \rightarrow 3\gamma$? The former background is potentially much larger. Suppose we observe a 14 GeV photon from the $e^+e^- \gamma$ process at $\theta = 20°$. The P_t of this photon will be balanced by the $e^\pm$ which radiated it. To a reasonable approximation we can write

$$\tan\theta_{e\pm} \simeq \theta_{e\pm} = \frac{E_\gamma \sin 20°}{E_{e\pm}} \simeq 6° \quad .$$

In other words there is a minimum angle, θ_{min}, beyond which one must see an electron (or positron) if one sees the 14 GeV photon with $20° < \theta < 160°$. The real kinematics and cross section appear in figure 29. With a veto for the $e^\pm$ down to $\theta = 6°$, the signal to noise would be 40:1.

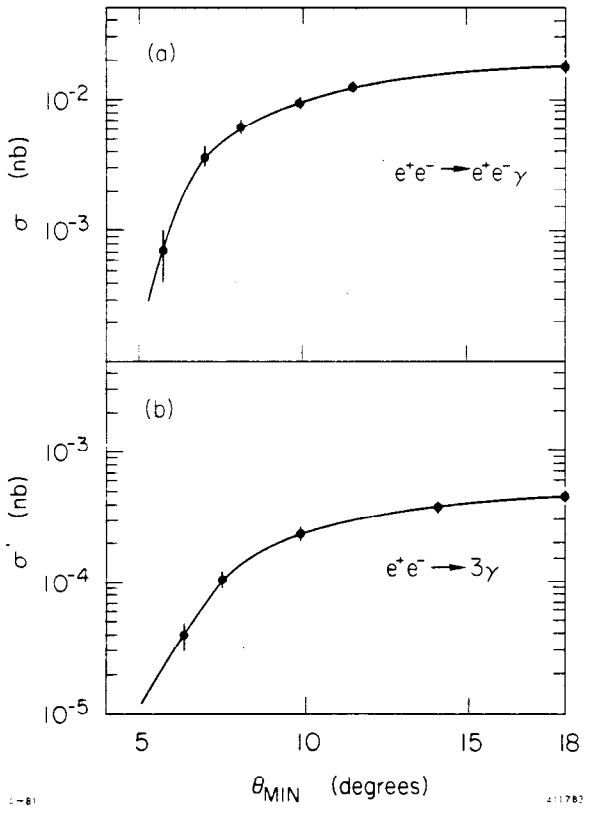

Fig. 29. Estimates of the backgrounds from the processes $e^+e^- \rightarrow e^+e^-\gamma$ and $e^+e^- \rightarrow 3\gamma$ as a function of $\theta_{\min}$ for $|y| \leq 0.94$ and $E_\gamma = 14.5 \pm 2.5$ GeV.

The detector required for this experiment is relatively simple. Electromagnetic shower counters down to within 6° of the beamline and a charged particle tracker (no magnet needed) for $20° < \theta < 160°$ to ensure that the γ is not an electron. All the SLC and LEP detectors are equipped to do this experiment.

There is nothing magic about the $E_{c.m.}$ chosen in the example of reference 30. In a recent study, the MARK II Group have decided that they are sufficiently well instrumented to run at about 4 GeV above the Z^0 peak. At this energy, the cross-section is about a factor of 2.5 times larger than at $E_{c.m.} = 105$ GeV.

This ν counting experiment is not that difficult to do experimentally. The main limitation will come from the need for a high luminosity machine. Without an average luminosity of $\gtrsim 10^{30}$ cm^{-2} sec^{-1} the search will be rate limited. There is also an important theoretical point to be made. One doesn't only count N_ν but

rather contributions from all neutral, stable, particles which couple weakly to the Z^0. If SUSY is correct, then $Z^0 \to \bar{\nu}_s \nu_s$ will contribute to this rate. We will see in the next sub-section that this potential contribution is, in all likelihood, considerably less than the contribution from one ν species ($\simeq 0.2 N_\nu$).

7.3 SUPERSYMMETRY

Since John Ellis's lectures at this School were devoted to this topic, I provide here a sketchy outline of the value of the Z^0 machines for testing SUSY. Also reference 32 by Kane and Haber is an excellent primer for the uninitiated. There are many models and many decay schemes and what I write down here is presumably true in some model(s). But this doesn't mean that it is correct – *i.e.* SUSY doesn't demand it, rather the model does.

Production cross sections for the partners of the normal fermions are characteristic of scalars namely

$$R_{\tilde{s}\bar{\tilde{s}}} = \frac{1}{4} R_{f\bar{f}} \quad .$$

Here $\tilde{s}$ indicates a SUSY scalar whose normal partner is denoted by f. However there are two SUSY partners for each normal fermion so in reality

$$R_{\tilde{s}\bar{\tilde{s}}} = \frac{1}{2} R_{f\bar{f}}$$

and

$$\frac{d\sigma_{\tilde{s}\bar{\tilde{s}}}}{d\cos\theta} = \frac{1}{2}\beta^3 \sin^2\theta \sigma_{f\bar{f}} \quad .$$

So, if $M_{\tilde{s}} < M_Z/2$, SUSY scalars could add significantly to the width of the Z^0. As we said previously, if Γ_Z is too wide there could be many reasons for it. One would have to search for each possibility separately.

Scalar leptons with $M_{\tilde{e}} < M_Z/2$ will be copiously produced and $B(Z^0 \to \tilde{\ell}^+\tilde{\ell}^-) = 1\frac{1}{2}\%\ \beta^3$ where β is the scalar lepton velocity. Presumably $\tilde{\ell}^\pm \to \ell^\pm\ \tilde{\gamma}$ and, assuming the $\tilde{\gamma}$ is stable, one gets a very distinctive signature namely events at the Z^0 which have two high energy leptons (e^+e^- , $\mu^+\mu^-$ or $\tau^+\tau^-$) with large missing P_t and energy. The presence of a stable light particle ($\tilde{\gamma}$) in the decay chains of all the SUSY particles implies that SUSY events are characterized by missing P_t and energy. This is a key element in the search for SUSY signatures.

— For scalar quarks $B(Z^0 \to \tilde{u}\bar{\tilde{u}}) = 6.6\%\ \beta^3$, $B(Z^0 \to \tilde{d}\bar{\tilde{d}}) = 5.3\%\ \beta^3$ where β is the quark velocity. The scalar quark will decay to a quark and a gluino or $\tilde{\gamma}$ and hence one has events with two jets which are not back to back but have substantial missing P_t and energy. Again this is a distinctive signature and, provided β is not too small, there is copious production.

For scalar neutrinos $B(Z^0 \to \tilde{\nu}\,\tilde{\bar{\nu}}) = 3\%\ \beta^3$ where β is the $\tilde{\nu}$ velocity. In order to discuss this channel further requires a decay scheme for the $\tilde{\nu}$. The schemes are complicated by the fact that one has no idea of the scalar electron, scalar $\nu, \ldots$ masses. Certainly a prominent decay mode will be $\tilde{\nu} \to \nu\tilde{\gamma}$ which is an invisible mode which could have a branching fraction $\simeq 0.6$. There are also multiple charged particle modes possible as known in figure 30 taken from Barnett et al.[33] How much will $Z^0 \to \tilde{\nu}\,\tilde{\bar{\nu}}$ contribute to the ν counting experiment? The contribution per SUSY species relative to a ν species will be

$$N_{\tilde{\nu}}/N_\nu = B^2(\tilde{\nu} \to \nu\tilde{\gamma})\ \frac{\Gamma(Z^0 \to \tilde{\nu}\,\tilde{\bar{\nu}})}{\Gamma(Z^0 \to \nu\bar{\nu})} \approx 0.2$$

where I have used $B(\tilde{\nu} \to \nu\tilde{\gamma}) \simeq 0.4$. In all likelihood then, it will be hard to see a scalar ν species in the neutrino counting experiment. However the possibility that scalar neutrinos exist could place systematic limits on how well one would measure N_ν.

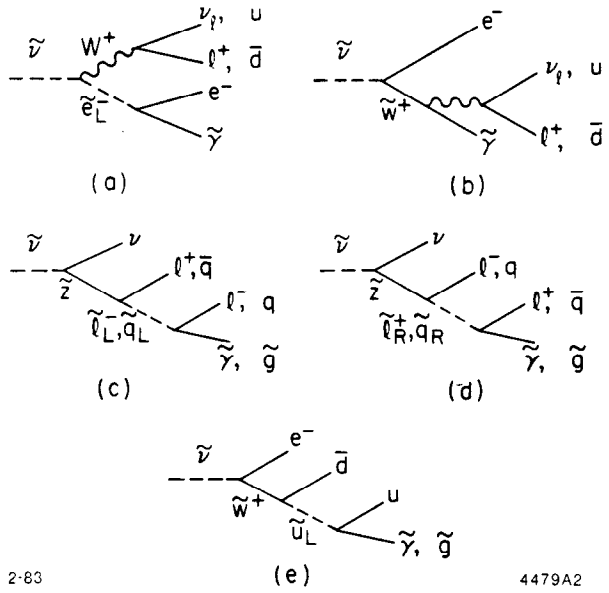

Fig. 30. Possible decay modes for $\tilde{\nu} \to$ multiple charged particles taken from the model of Barnett *et al.*, reference 33.

The multicharge decays shown in figure 30 could generate some spectacular events at Z^0. The topology

$$Z^0 \to \tilde{\nu}\,\tilde{\bar{\nu}} \begin{cases} \to \nu_e e^- e^+ \tilde{\gamma} \\ \to \nu\tilde{\gamma} \end{cases}$$

would yield an electron and positron in one hemisphere of the detector and nothing else! Even if $B(\tilde{\nu} \to \nu_e e^+ e^- \tilde{\gamma}) \approx 10^{-3}$, 10^6 Z^0's would yield ~ 40 such events! Another interesting topology would be

$$Z^0 \to \tilde{\nu}\,\tilde{\bar{\nu}}$$
$$\quad \to e^- q\bar{q}\tilde{g}$$
$$\quad \to \tilde{\gamma}\nu$$

yielding an electron, two quark jets and a gluino in one hemisphere and nothing visible recoiling against them. The electron energy is expected to be large ($\langle P_e \rangle \approx$ 8 GeV) making them easy to detect. Certainly, if SUSY is correct, there is a chance that we could see some spectacular events at the Z^0 .

What about the charginos $\omega^\pm$, $h^\pm$ which are the spin 1/2 partners of the $W^\pm$ and $H^\pm$. Since they couple weakly, these particles look like heavy leptons $L^\pm$ discussed earlier. They decay via

$$h^\pm, w^\pm \to W^\pm \tilde{\gamma}$$
$$\quad \to \ell^\pm \nu \text{ or } q\bar{q} \quad .$$

The decay will be the same as $L^\pm \to W^\pm \nu$ except for effects arising from large $\tilde{\gamma}$ mass. How are they distinguished from $L^\pm$? Consider for the moment the unmixed case for which the weak couplings are

$$v = (T_{3L} + T_{3R} - 2Q \sin^2 \theta_W)$$

$$a = T_{3L} - T_{3R}$$

with

$$T_{3L} = T_{3R} = \pm 1 \qquad \text{for } w^\pm$$

$$T_{3L} = T_{3R} = \pm 1/2 \quad \text{for } h^\pm \ .$$

Hence $v_{W^\pm} = 1.56$, $v_{h^\pm} = 0.56$ and $a_{w^\pm} = a_{h^\pm} = 0$. So for this unmixed case

$$\frac{\Gamma(Z^0 \to w^+ w^-)}{\Gamma(Z^0 \to \tau^+ \tau^-)} = 9.6$$

and

$$\frac{\Gamma(Z^0 \to h^+ h^-)}{\Gamma(Z^0 \to \tau^+ \tau^-)} = 1.2 \quad .$$

Hence, if less massive than $M_Z/2$, charginos could add as much as $\sim 33\%$ to Γ_Z. The search for $w^\pm$, $h^\pm$ proceeds exactly as the search for $L^\pm$ discussed earlier.

How does one distinguish the $L^{\pm}$ from the $w^{\pm}$, $h^{\pm}$? Their weak interactions are very different! The charge asymmetry is

$$A_{F-B} = \frac{3v_e a_e v_f a_f}{(v_e^2 + a_e^2)(v_f^2 + a_f^2)}$$

$$= 4.3\% \text{ for } L^{\pm}$$

$$= 0 \text{ for } w^{\pm},\ h^{\pm} \text{ in unmixed cases.}$$

We have considered the simplest unmixed case. Suppose the $w^{\pm}$ and $h^{\pm}$ are maximally mixed in states $\tilde{w}_1$ and $\tilde{w}_2$. Then

$$\frac{\Gamma(Z^0 \to \tilde{w}_1^+ \tilde{w}_1^-)}{\Gamma(Z^0 \to \tau^+\tau^-)} = \frac{\Gamma(Z^0 \to \tilde{w}_2^+ \tilde{w}_2^-)}{\Gamma(Z^0 \to \tau^+\tau^-)} = 5.5$$

and

$$A_{F-B}^{\tilde{w}_1} = 14\%$$

$$A_{F-B}^{\tilde{w}_2} = -14\% \quad .$$

Of course we have no guidance from the theory as to what level of mixing, if any, there is.

7.4 Models with Extended Electro-Weak Gauge Groups: $SU(2) \wedge U(1) \wedge \mathcal{G}$

At low Q^2, the effective Hamiltonian of the Standard Model for charged current interactions is given by

$$H_{cc} = \frac{4\mathcal{G}_F}{\sqrt{2}} J_\mu^+ J_\mu^-$$

and for neutral current interactions by

$$H_{NC} = -\frac{e^2}{q^2} J_{em}^2 + \frac{4\mathcal{G}_F}{\sqrt{2}} \left\{ \left(J^3 - \sin^2\theta_W J_{em} \right)^2 \right\}$$

where (J^+, J^-, J^3) form the weak isospin current. The success of the Standard Model at low energies is testament to the validity of this current-current description. Neither neutrino scattering experiments nor the e-d parity violation

experiment probe the electromagnetic part of the weak current. Hence we can add to H_{NC}

$$H'_{NC} = -\frac{e^2}{q^2}\, J^2_{em} + \frac{4\mathcal{G}_F}{\sqrt{2}} \left\{ \left(J^3 - \sin^2\theta_W J_{em} \right)^2 + C J^2_{em} \right\}$$

without conflicting any of the low energy experimental data. The only low energy bound for C is $C < 4$ which comes from measurements of the anomalous magnetic moment of the muon.

The lepton pair charge asymmetry measurements at PETRA and PEP probe the term CJ^2_{em} via the interference of the weak and electromagnetic propagators. However these measurements do not place stringent limits on C. The freedom implied by the addition of the term CJ^2_{em} permits models which extend the Electro-Weak gauge group to $SU(2) \wedge U(1) \wedge \mathcal{G}$. Examples of such models are $SU(2) \wedge U(1) \wedge U(1)'$ (references 34,37), $SU(2) \wedge U(1) \wedge SU(2)'$ (reference 35) and $SU(2)_L \wedge SU(2)_R \wedge U(1)$ (references 36,37). The common feature of these models is the presence of two Z^0's with $M_{Z_1} < M_{Z^0} < M_{Z_2}$ where M_{Z^0} is the mass of the Z^0 in the Standard Model. The reason why one gets two energy levels is that CJ^2_{em} can be thought of as a perturbation and this perturbation splits the single energy level (M_{Z^0}). We discuss briefly some models for which $\mathcal{G} = U(1)$ and $SU(2)$, to illustrate how the formalism works.

In the model discussed in reference 34 in which $\mathcal{G} = U(1)$, all fermions transform under $SU(2) \wedge U(1)$ in the usual manner and they are invariant under $U(1)'$. The spontaneous symmetry breaking is achieved using a pair of complex Higgs fields, ϕ_1 and ϕ_2. The Higgs field ϕ_1 follows the Standard Model prescription. However, ϕ_2, which is invariant under $SU(2)$, has non-trivial transformations under $U(1) \wedge U(1)'$. Hence we recover the same $W^{\pm}$ structure as in the Standard Model. However ϕ_2 gives rise to an additional heavy neutral boson which can be associated with $U(1)'$. We thus obtain

<u>for $U(1)$</u>

$$(e^-, \nu_e) \begin{pmatrix} V_0 & 0 \\ 0 & V_0 \end{pmatrix} \begin{pmatrix} e^- \\ \nu_e \end{pmatrix}$$

<u>for $SU(2)$</u>

$$\overline{} \\ (e^-, \nu_e) \begin{pmatrix} W^0 & W^- \\ W^+ & W^0 \end{pmatrix} \begin{pmatrix} e^- \\ \nu_e \end{pmatrix}$$

<u>Standard Model</u>: $SU(2) \wedge U(1)$

$$(\gamma, Z^0) = \begin{pmatrix} \cos\theta & -\sin\theta_W \\ \sin\theta_W & \cos\theta_W \end{pmatrix} \begin{pmatrix} V^0 \\ W^0 \end{pmatrix};$$

one parameter, $\sin^2\theta_W$

and for $U(1)'$

$$(e^-, \nu_e) \begin{pmatrix} V_0' & 0 \\ 0 & V_0' \end{pmatrix} \begin{pmatrix} e^- \\ \nu_e \end{pmatrix}$$

$SU(2) \wedge U(1) \wedge U(1)'$

$$(\gamma, Z_1, Z_2) = (3 \times 3) \begin{pmatrix} V_0 \\ V_0' \\ W_0 \end{pmatrix};$$

three parameters .

The three parameters of $SU(2) \wedge U(1) \wedge U(1)'$ can be taken as $\sin^2 \theta_W$, M_1 and M_2. The parameter C is given by

$$C\,(\mathcal{G} = U(1)) = \cos^4 \theta_W \left(\frac{M_{Z^0}^2}{M_1^2} - 1\right)\left(\frac{M_{Z^0}^2}{M_1^2} - 1\right)$$

so as either $M_{1,2} \to M_{Z^0}$ we recover the Standard Model with $C = 0$.

In the model with $\mathcal{G} = SU(2)$[35] one goes through a similar procedure but in this instance ϕ_2 has non-trivial transformations under $SU(2) \wedge SU(2)'$. Again one obtains two neutral heavy bosons. In this model

$$C\,(\mathcal{G} = SU(2)) = \sin^2 \theta_W \left(\frac{M_{Z^0}^2}{M_1^2} - 1\right)\left(\frac{M_{Z^0}^2}{M_1^2} - 1\right)$$

and again $C = 0$ as $M_{1,2} \to M_{Z^0}$.

How does one test for these extended Electro-Weak gauge groups at the Z^0 energy range? Inspection of the modified H'_{NC} will convince you that in essence the extra CJ_{em}^2 term has the effect of modifying the value of what we measure for $\sin^2 \theta_W$. As we discussed previously, the most sensitive measure of $\sin^2 \theta_W$ comes from looking at the left-right asymmetry A_{LR}. Shown in figure 31 is A_{LR} as a function of $E_{c.m.}$ for the Standard Model and for $SU(2) \wedge U(1) \wedge U(1)'$ in which $\sin^2 \theta_W$ is taken to be 0.22. Running at the Z^0 pole one would easily see the deviation from the Standard Model. However one will have to run at a substantially higher $E_{c.m.}$ in order to get sensitivity to M_2. Although not discussed here in detail, we show the sensitivity of A_{LR} to tests for the model $SU(2)_L \wedge SU(2)_R \wedge U(1)$.[36] Figure 32 shows A_{LR} as a function of $E_{c.m.}$ for the Standard Model and the left-right symmetric model.[7] In this case running at the nominal Z^0 mass can distinguish the extended model from the Standard Model and yield the mass of the second heavy boson. This is shown more explicitly in figure 32b.

Another example comes from superstring models which add a $U(1)$ group to the Standard gauge structure thereby producing as second Z^0-like particle. Tests of models of this type using polarized electrons at the Z^0 are discussed in great detail in reference 37. As an illustration we show one figure from these

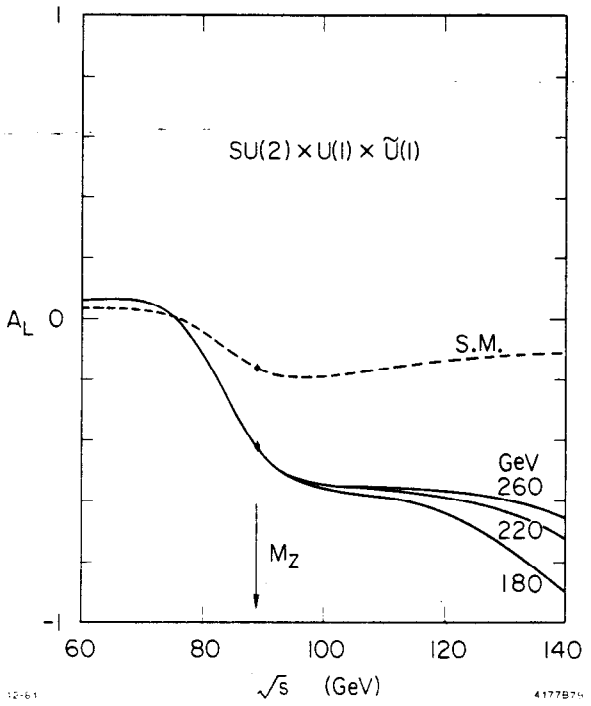

Fig. 31. A_{LR} as a function of $\sqrt{s}$ calculated in the Standard Model (S.M.) and in a $SU(2) \times U(1) \times \tilde{U}(1)$ model for different values of the mass of the second neutral boson. The two data points indicate the statistical accuracy expected for 3×10^4 Z^0 decays.

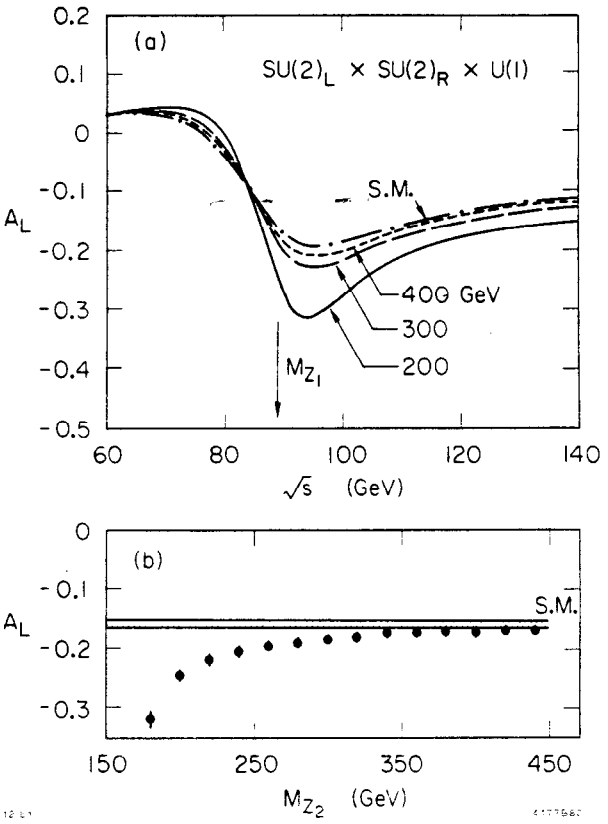

Fig. 32. A_{LR} calculated in the Standard Model (S.M.) and in the $SU(2)_L \times SU(2)_R \times U(1)$ model; (a) as a function of $\sqrt{s}$ and for different values of the mass of the second neutral boson; (b) at $\sqrt{s} = M_Z$, comparison of the A_{LR} value in the Standard Model and in the $SU(2)_L \times SU(2)_R \times U(1)$ model as a function of the mass of the second neutral boson for 3×10^4 Z^0 decays.

authors (figure 33) which shows A_{LR} as a function of $M_{Z'}/M_Z$ for two parameter choices in a generalized superstring type model. For comparison the Standard Model value for A_{LR} is obtained from the figure by letting $M_{Z'}/M_Z \to \infty$. Considerable sensitivity to high mass Z''s would be obtained – for the high (low) resolution polarimeter, A_{LR} will be measured to 1% (5%) at the SLC.

From the above examples, it is clear that polarized beams at the SLC provide an important tool for searching for Nature's correct gauge group.

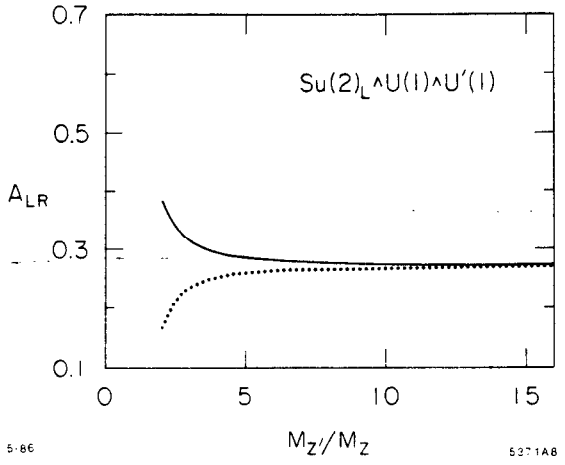

Fig. 33. A_{LR} on the Z^0 resonance as a function of $M_{Z'}/M_Z$ for two parameter choices of a superstring model as discussed in reference 37. The Standard Model value of A_{LR} is obtained by letting $M_{Z'}/M_Z \to \infty$.

8. PHYSICS ABOVE THE Z^0, THE LEPII AND LEPIII FRONTIER

There is considerable physics which can be studied using the LEPII machine ($E_{c.m.} \leq 170$ GeV) and the LEPIII machine ($E_{c.m.} \lesssim 250$ GeV). This program is thoroughly discussed in reference 2. In these lectures, given the constraints of time, just a few topics were chosen for discussion. Many of them relate to the kinds of tests which were discussed for Z^0 running.

8.1 Searches for New Charged Fermions

For all new fermion searches, we were limited at the Z^0 to masses $< M_{Z^0}/2$. At LEPII the limiting masses for these searches are $E_{c.m.}/2$. Hence LEPIII provides considerable improvement in search domains. However we must now consider that the production cross-sections are much smaller and in order to perform these searches will require good luminosity and considerable running time.

The most basic measurement one can perform is a measurement of $R = \sigma_{\text{hadrons}}/\sigma_{\text{point}}$ as discussed in section 4. Using formula (4) in section 4, one can calculate R for $S > M_Z^2$. In the limit $S \gg M_Z^2$ ($E_{c.m.} > 200$ GeV) R is independent of S and for 5 quarks has a value $R_5 \sim 7$ for $\sin^2\theta_W = 0.22$. For $S < 200$ GeV one still sees the effects of the Z pole – at the highest LEPII energy of 170 GeV $R_5 = 10.4$, at 150 GeV $R_5 = 12.2$. Can we use a measurement of R to search for new quarks at LEPII? The increase in (δR_t) from a t quark at $E_{c.m.} = 160$ GeV is about 2.4 or 25% of R_5, where I have ignored finite quark mass effects (*i.e.* threshold effects). The increase for a b type quark is 1.72 or 17% of R_5. Typical systematic errors are at the $\sim 3\%$ level for R measurements, so the

measurements will not be systematics limited. However in order to establish a 4σ effect in R will take good average luminosity. In addition, because of the close proximity of the large cross section at $E_{c.m.} = M_{Z^0}$, radiative corrections will be very important. They will probably raise R_5 considerably, while not raising $\delta R_{t,b'}$ nearly as much. This could make this measurement very difficult.

Assuming $\langle \mathcal{L} \rangle = 5 \times 10^{30}$ cm^{-2} sec^{-1}, one finds that $R = 10.4$ ($E_{c.m.} =$ 170 GeV) corresponds to 15 hadronic events/day. Hence to see a 4σ effect for $t\bar{t}$ ($b'\bar{b}'$) production would take 17 (25) days.

Presumably these heavy quark events will have an event shape which is easily distinguishable from the light quark decays as we discussed for the Z^0 searches. A search based on event shapes would also suffice to establish the presence of a new heavy quark.

A new heavy lepton will show up in the low multiplicity events which would not, of course, satisfy the requirements for hadronic events. Production will be via $e^+e^- \to L^+L^-$. The simplest way to look for a new heavy lepton will be to search for non-coplanar ex, μx and $e\mu$ events. The same event types will be produced by $\tau^+\tau^-$ events – however because the τ is so light compared to $E_{c.m.}$ the events would be coplanar. We recall from section 7.2 that $B(L^+ \to e, \mu) = 8\%$ and therefore:

$$\#\ ex \text{ events/day} = 0.2\ \beta_L(3-\beta)L^2)/2$$

where β_L is the heavy lepton velocity and I have assumed $\langle \mathcal{L} \rangle = 5 \times 10^{30}$ cm^{-1} sec^{-1} and $E_{c.m.} = 170$ GeV. Adding both the ex and μx events and having a little patience, one would be able to search for a new heavy lepton. Above the W^+W^- threshold, care will have to be taken to account for the background from this channel.

From these too examples one sees how crucial the peak luminosity for LEPII,III will be. Without $\mathcal{L} \sim 10^{31}$ cm^{-2} sec^{-1} useful physics will be hard to come by. But given good luminosity one will be able to search for new quarks and charged leptons up to masses $\lesssim E_{\text{beam}}$.

8.2 SEARCHING FOR H^0, $H^\pm$

What about searching for H^0? As discussed in John Ellis's lectures at this School, the best search procedure will be via the process

$$e^+e^- \to Z^{0*} \to Z^0\, H^0$$

as depicted in figure 34. The total cross section for this process is given by (see

reference 2, volume II)

$$\sigma(e^+e^- \to Z^0H^0) = \frac{\pi\alpha^2 P_Z[3M_Z^2 + P_Z^2][1 + (1 - 4\sin^2\theta_W)^2]}{24\sin^2\theta_W \cos^4\theta_W \sqrt{S}\,(S - M_Z^2)^2}$$

where P_Z is the Z^0 momentum

$$P_{Z^0} = \frac{1}{2}\left[S - 2M_Z^2 - 2M_H^2 + S^{-1}\left(M_Z^2 - M_H^2\right)^2\right]^{1/2} \quad .$$

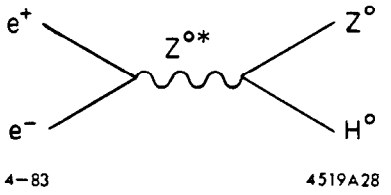

Fig. 34. The process $e^+e^- \to Z^{0*} \to Z^0H^0$.

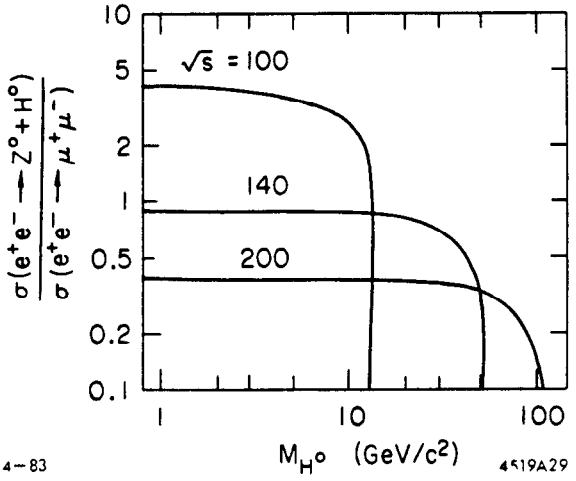

Fig. 35. The rate for the process $e^+e^- \to Z^0H^0$ is shown as a function of $E_{c.m.}$ and M_{H^0}. The rate is normalized to the point cross section which has the value $86.8/E_{c.m.}^2$ nb.

This cross section is plotted in figure 35 as a function of M_{H^0} for three choices of $E_{c.m.}$. For a given $E_{c.m.}$, the cross section is relatively constant as a function of M_{H^0}, falling rapidly as the kinematic limit of $(E_{c.m.} - M_{Z^0})$ is reached. For $\langle\mathcal{L}\rangle = 5 \times 10^{30}$ cm^{-2} sec^{-1} the event rate is ~ 0.8 event/day at $E_{c.m.}$ of 170 GeV with a maximum search mass of $\lesssim 70$ GeV/c^2. So in a year one would have ~ 300 events in total. The corresponding event rate at $E_{c.m.} = 140$ GeV would be ~ 800 with a maximum search mass of 40 GeV/c^2. We should recall here that LEPI and SLC will have a maximum search mass at $E_{c.m.} = M_{Z^0}$ of $\lesssim 40$ GeV. So LEPII,III has a sizeable advantage in search mass. However the rates are low. Realistically to search for these events one would have to require that the Z^0 decay to e^+e^- or $\mu^+\mu^-$. One has the Z^0 constraint plus two identified leptons which will provide a clean signal. The H^0 mass would result from calculating

the mass recoiling against the Z^0 decay products. Requiring the leptonic decay channels will cost a factor of 16 in rate. With larger $E_{c.m.}$ this will cause severe statistics problems – in that case one would have to try to augment these clean channels with $Z^0 \to \nu\bar{\nu}$, $\tau^+\tau^-$ and $q\bar{q}$.

How about searching for $H^\pm$ at LEPII,III? The production cross section for $e^+e^- \to H^+H^-$ is given by

$$\sigma_{H^+H^-} = \frac{1}{4}\,\beta^3_{H^\pm}\,\sigma_{\mu^+\mu^-}$$

where $\sigma_{\mu^+\mu^-}$ is not the point cross section but also has a contribution coming from the Z^0 propagator. (To get an exact value of this cross section one can evaluate equation (4) in section 4.) $\sigma_{\mu^+\mu^-}$ has the value of ~ 4 pb at $E_{c.m.} = 170$ GeV and ~ 1.5 pb at $E_{c.m.} = 250$ GeV. So roughly speaking H^+H^- production is about 5% of the continuum $e^+e^- \to$ hadrons. To detect the presence of the H^+H^- will require reconstructing four jet events. The QCD background will be present at a level of roughly half the H^+H^- signal (for $\beta = 1$). The two sources can be distinguished by their production angular distribution – $\sin^2\theta$ for the H^+H^- $(1 + \alpha\cos\theta + \cos^2\theta)$ for the QCD events. Event rates will be ~ 400 H^+H^- events per year for $\langle\mathcal{L}\rangle = 5 \times 10^{30}$ cm^{-2} sec^{-1} and $E_{c.m.} = 170$ GeV. With sufficient running searches for $H^\pm$ up to energies $\lesssim E_b$ should be possible at LEPII,III.

8.3 $e^+e^- \to W^+W^-$

LEPII and III are by far the best place to study W^+W^- production. The three lowest order diagrams which contribute to this process are shown in figure 36 and the resulting cross section as a function of E_b is shown in figure 37. We see that once above threshold the cross-section is roughly constant in the LEPII,III energy range and is also large ($\sim$ 3000 W^+W^- per year for $\langle\mathcal{L}\rangle = 5 \times 10^{30}$ cm^{-2} sec^{-1}). Besides providing a valuable laboratory for studying $W^\pm$ decays, LEPII also provides the only place to study the gauge couplings γW^+W^- and $Z^0W^+W^-$, thus making a unique contribution to testing the Standard Model. The form of the cross section shown in figure 37 is crucially determined by cancellations among the three competing lowest order diagrams (figure 36). In particular, the ν exchange diagram would grow without bound as $E_{c.m.}$ increases unless moderated by the two other graphs. Hence a measure of

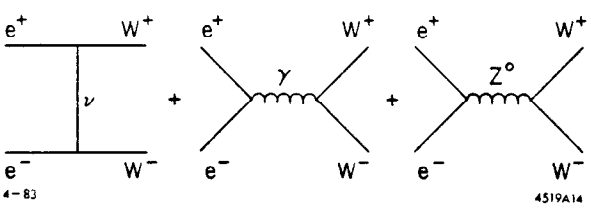

Fig. 36. The three processes which contribute to $e^+e^- \to W^+W^-$.

the total W^+W^- cross section provides a crucial test of the Standard Model. A precise check will require knowledge of weak radiative corrections. However SLC and LEPI should provide an excellent understanding of these effects and, in all likelihood, we will know how to include these effects.

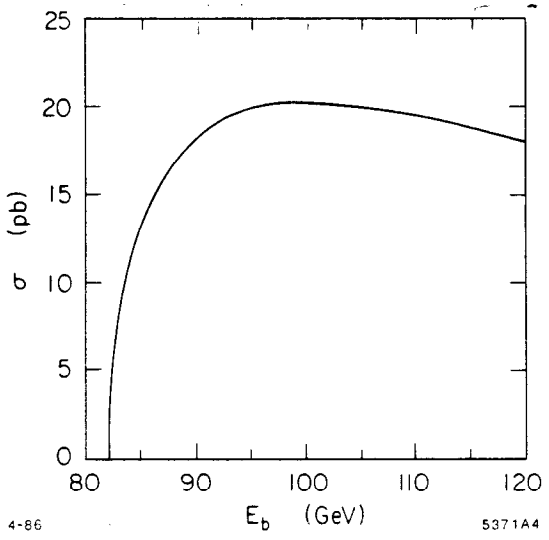

Fig. 37. The cross section for $e^+e^- \rightarrow W^+W^-$ as a function of beam energy. LEPII has a maximum beam energy of 85 GeV.

What do the events look like. The $W^\pm$ coupling strength is democratic with respect to fermions and hence for $N_G = 3$ generations

$$\frac{B(W \rightarrow \ell\nu)}{B(W \rightarrow \text{all}} \simeq \frac{1}{4N_G} = 8\%$$

and

$$\frac{B(W \rightarrow q'\bar{q})}{B(W \rightarrow \text{all}} \simeq 25\% \; |V_{qq'}|^2$$

where $V_{qq'}$ is the Kobayashi-Maskawa weak mixing matrix element and where for $q = t$ finite mass effects are important. For $W \rightarrow tb$ with $M_t = 40$ GeV/c^2 $B(W \rightarrow \bar{t}q) \simeq 18\% \; |V_{tq}|^2$. Hence W^+W^- decays predominantly to 4 jets (76%) with little background from $e^+e^- \rightarrow 4$ jets where we can estimate the cross section to be $\alpha_s^2 R\sigma_{\text{point}} \approx 0.6$ pb at $E_{c.m.} = 170$ GeV. For an average luminosity of 5×10^{30} cm^{-2} sec^{-1} one would get six 4 jet events and one $\ell^\pm q\bar{q}'$ per day from W^+W^- production. Both of these provide clean topologies for the study of $W^\pm$.

How well could we measure the $W^\pm$ mass? The $p\bar{p}$ measurements are limited to $\sim$ 2 GeV errors because of the inability of the calorimeters to reconstruct

all the jet energy. This problem can be overcome at LEPII,III because one can use E_b as a constraint for $E_{W^\pm}$ thereby removing this limitation. As an example figure 38 shows the di-jet mass (2 entries per event) reconstructed in a LEP study (reference 2, volume 2) for $E_b = 100$ GeV. From this study an error of $\lesssim 150$ MeV/c^2 is obtained for the W mass. Other methods which could be used are a fit to the threshold curve (figure 37) or a study of the endpoint of the electron momentum spectrum arising from $W \rightarrow e\nu$ decays. With high probability then, an order of magnitude improvement in our knowledge of M_W should be achieved at LEPII.

As a final example of what can be achieved at LEPII,III we remind ourselves that whenever we increase $E_{c.m.}$ we are able to probe increasingly smaller characteristic fermion sizes. If fermions were not point-like, their production via $e^+e^- \rightarrow ff$ would be characterized by an intrinsic mass scale Λ such that $\langle r \rangle \sim 1/\Lambda$. These scales introduce so-called contact terms which modify the production cross-sections predicted by the Standard Model. The simplest case to consider is Bhabha scattering $e^+e^- \rightarrow e^+e^-$. Studies by the LEP groups[2] indicate that limits on compositeness down to $\langle r \rangle \sim 10^{-18}$ cm should be possible for electrons.

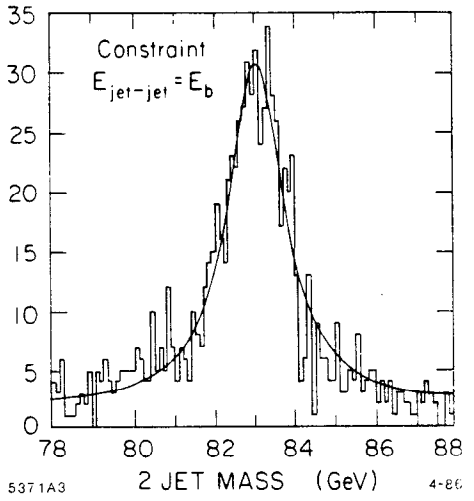

Fig. 38. Di-jet mass for events simulated as $e^+e^- \rightarrow W^+W^-$. A clear $W^\pm$ peak is seen. This simulation was done for the LEP study (see reference 2).

Because of the constraints of time, all the physics of LEPII and LEPIII have not been covered here. But enough examples have been chosen to indicate that this will be a rich and fruitful physics frontier.

9. CONCLUSIONS

As outlined in section 2, e^+e^- interactions have served the physics community well, providing many crucial discoveries and a large body of rich experimental data. The future for e^+e^- interactions with the imminent turn-on of SLC and LEP promises to continue this tradition with the very real possibility of new discoveries and the certain program of diverse and important measurements.

ACKNOWLEDGEMENTS

I spent a most enjoyable week at Lake Louise for what was their inaugural Winter School. They are to be congratulated on a fine School. I learnt much from my co-lecturers and enjoyed enormously the warm hospitality of our Canadian hosts. I thank the organizers for including me in their program. I also wish to thank the staff at SLAC who prepared this document despite my constant tardiness.

REFERENCES

1. (a) e^+e^- *Interactions at Very High Energy: Searching Beyond the Standard Model*, SLAC-PUB-3093 and Proceedings of the 1982 SLAC Summer Institute on Particle Physics. (b) Z^0 *Decay Modes – Experimental Measurements*, SLAC-PUB-3407 and Proceedings of the 1984 Theoretical Advanced Study Institute on Elementary Particle Physics.
2. Physics at LEP, edited by John Ellis and Roberto Peccei, CERN86-02, Volumes 1 and 2.
3. R. Hollebeek, Nucl. Instrum. Methods **184**, 333 (1981).
4. ECFA 81/54, General Meeting on LEP, Villars-sur-Ollon, Switzerland, June 1981.
5. *SLAC Linear Collider Conceptual Design Report*, SLAC-299 (June 1980); B. Richter, SLAC-PUB-2854 (1981).
6. S. Ozaki, Proceedings of the 1981 International Symposium on Lepton and Photon Interactions at High Energies, Bonn, 1981, p. 935.
7. C.Y. Prescott, SLAC-PUB-2854 (1981); Proceedings of the SLC Workshop, SLAC-247 (March 1982).
8. For a derivation of this cross section and most of the formulae quoted in this chapter see C. Quigg, *Gauge Theories of the Strong, Weak and Electromagnetic Interactions.*
9. J.D. Jackson and D. Scharre, Nucl. Instrum. Methods **128**, 13 (1975).
10. W. Marciano and A. Sirlin, Phys. Rev. **D22**, 2695 (1980); M. Veltman, Phys. Lett. **91B**, 95 (1980).
11. (a) CERN Yellow Reports 76-18 (1976) and 79-01 (1979). (b) Proceedings of the SLC Workshop on Experimental use of the SLC; SLAC-247 (1982). (c) Proceedings of the Cornell Z^0 Theory Workshop; CLNS 81-485.

12. LEP Detectors:
OPAL CERN/LPC/83-4
L3 CERN-Proposal-LEP-L3
ALEPH CERN/LPC/83-2
DELPHI DELPHI-83-66/1
SLC Detectors:
MARK II SLAC-PUB-3561/CALT-68-1015
SLD SLD Design Report.

13. Particle Data Group, Rev. Mod. Phys. **56** (1984).

14. UA2 Collaboration, Z. Phys. **C30**, 1 (1986).

15. MARK II Collaboration, *Proposal for Precise Beam Energy Measurement at the SLC.*

16. Y.-S. Tsai, Phys. Rev. **D4**, 2821 (1971).

17. H. Ogren *et al.*, *Polarization at the SLC: A Study by the SLC Polarization Group.*

18. G. Hanson *et al.*, Phys. Rev. Lett. **35**, 1609 (1975).

19. G. Hanson, Data taken from interim report at the MARK II Collaboration Asilomar Workshop, March 1986.

20. G. Tarnopolsky, SLAC-PUB-2842 (1981).

21. L.B. Okun, Proceedings of the 1981 International Symposium on Lepton and Photon Interactions at High Energy, Bonn, 1981, p. 1018.

22. J.D. Bjorken, SLAC-198 (1976).

23. J. Finjord, Physica Scripta, Vol. **21**, 143 (1980).

24. W. Marciano *et al.*, Phys. Rev. Lett. **43**, 22 (1979); D. Albert *et al.*, Nucl. Phys. **B166**, 460 (1980).

25. See for instance J.M. Dorfan, Proceedings of the 1983 International Symposium on Lepton and Photon Interactions at High Energies, Cornell University, p. 686.

26. M.B. Einhorn and B.G. Weeks, Nucl. Phys. **B146**, 445 (1978); K. Shizuya and S.-H.H. Tye, Phys. Rev. Lett. **41**, 787 (1978).

27. For a summary see for instance G. Baranko, Proceedings of the International Europhysics Conference on High Energy Physics, Bari, Italy, July 1985, p. 226.

28. K. Hayes, *B Tagging at the SLC*, MARK II/SLC NOTE #73.

29. See for instance, Ling-Lie Chau, Brookhaven Print-85-0555, Invited talk at the Symposium on High Energy e^+e^- Interactions, Nashville, Tenn., April 1984 and APS Spring Meeting, Washing, D.C., April 1984.

30. G. Barbiellini *et al.*, Phys. Lett. **106B**, 414 (1981).

31. E. Ma and J. Okada, Phys. Rev. Lett. **41**, 287 (1978); K. Gaemers *et al.*, Phys. Rev. **D19**, 1605 (1979).

32. G. Kane and H. Haber, UM-HE-TH83-17.

33. M. Barnett *et al.*, SLAC-PUB-3224 (September 1983).

34. E.H. De Groot *et al.*, Z. Phys. **C5**, 127 (1980). This reference discusses the general question of $SU(2) \wedge U(1) \wedge G$.

35. V. Barger *et al.*, Phys. Rev. **D25**, 1384 (1982).

36. A. De Rujula *et al.*, Annals of Phys. **109**, 242,258 (1977).

37. M. Cvetič and B.W. Lynn, SLAC-PUB-3900 (March 1986).